Aquaculture 610 (2026) 742940

Contents lists available at ScienceDirect

Aquaculture

journal homepage: www.elsevier.com/locate/aquaculture

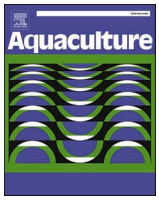

Pond aquaculture dynamics in Asia: Satellite time series for analyzing the spatio-temporal development of coastal aquaculture

Marco Ottinger [a,*], Kemeng Liu [b], Tobias Ullmann [b], Juliane Huth [a], Claudia Kuenzer [a,b], Felix Bachofer [a]

[a] German Aerospace Center (DLR), Earth Observation Center (EOC), German Remote Sensing Data Center (DFD), 82234 Wessling, Germany
[b] University of Wuerzburg, Institute of Geography and Geology, Department of Remote Sensing, 97074 Wuerzburg, Germany

ARTICLE INFO

Keywords:
Aquaculture
Ponds
Dynamics
Asia
Satellite time series
Landsat
Earth observation

ABSTRACT

Asia plays a dominant role in global aquaculture, contributing over 88 % of the total aquaculture output, primarily through pond aquaculture systems used for the farming of fish, shrimp, and mussels. Coastal regions in Asia have experienced rapid spatial expansion of pond aquaculture. Recognizing the importance of spatial data in effectively monitoring and managing these systems, we present a methodological approach utilizing dense optical satellite time series archive data to analyze the spatio-temporal development of coastal pond aquaculture in Asia. This study builds on previous work that delineated all aquaculture ponds at a single-pond level for the entire coastal zone using a multi-sensor Earth Observation approach, integrating both SAR and optical satellite data. The resulting continental-scale vector dataset of mapped aquaculture ponds served as reference to derive spatio-temporal dynamics of coastal aquaculture. By utilizing multi-decadal Landsat archive data (1984–2019), we developed a framework to determine the annual status of each pond based on water masks derived from satellite time series. The methodology was applied across 22 coastal countries in South Asia, East Asia and Southeast Asia to investigate the development patterns of pond aquaculture. Using the complete, continental-scale dataset on annual pond aquaculture status, this research conducted geostatistical analyses of growth rates and spatial expansion patterns across various administrative levels, including national and district scales. Growth dynamics were examined for each individual country at 5- and 10-year time intervals. Between the 1980s and 2019, coastal Asia experienced significant expansion of pond aquaculture in time and space, with China, Indonesia, India, Vietnam, and Thailand emerging as the largest contributors. In 1988, reference aquaculture ponds covered around 6500 km^2, increasing to over 19,000 km^2 in 2019, representing a more than three-fold increase. Among the examined countries, China maintained the largest pond aquaculture industry, accounting for 40.6 % of the total active pond area in 2019, followed by Indonesia (13 %) and India (11.2 %).

1. Introduction

Asia dominates the global aquaculture industry, accounting for 88 % of global production, equivalent to 80.3 million tonnes in 2021 (FAO, 2023), primarily through land-based pond aquaculture. The region's long-standing tradition of fish and shrimp farming in these ponds has underpinned Asia's central role in global aquaculture production (see Fig. 1). Overfishing, which has led to declining fish productions and stagnant catches, has further driven the growth of aquaculture to meet the rising demand for seafood (Akber et al., 2020; Naylor et al., 2021; Béné et al., 2016). Consequently, aquaculture has become the fastest-growing sector in the global food economy, now producing half of the world's consumable fish. The rapid expansion of aquaculture, particularly in Asia, highlights the importance of spatial survey data, continuous mapping, and environmental monitoring in advancing research and ensuring sustainable practices. In Southeast and East Asia, aquaculture has expanded rapidly since the 1990s, becoming a major industry and key driver of employment. However, this growth has raised concerns about environmental impacts, including water pollution, destruction of mangrove forests (Aslan et al., 2021; Herbeck et al., 2020; McSherry et al., 2023) and coastal wetlands (Ballut-Dajud et al., 2022), and occupation of ecological land (Zhang et al., 2022). Unregulated wastewater discharge is a significant issue, releasing high loads of nutrients and suspended solids into natural water bodies (Ahmed and

* Corresponding author.
E-mail address: marco.ottinger@dlr.de (M. Ottinger).

https://doi.org/10.1016/j.aquaculture.2025.742940
Received 9 August 2024; Received in revised form 29 January 2025; Accepted 6 July 2025
Available online 8 July 2025

Thompson, 2019; Dauda et al., 2019). To address these impacts, sustainable aquaculture practices, such as improved wastewater treatment and sustainable land use, are essential. Climate change also poses a significant challenge, with rising sea levels, increasing water temperatures, and acidification affecting yields and economic stability (Maulu et al., 2021). Spatial data and information are crucial for effective management and preservation of natural water resources. In light of these concerns, spatial information and data are crucial for effective management and preservation of natural water resources. (See Fig. 2.)

Satellite remote sensing is widely acknowledged for enabling large-scale, routine mapping and monitoring of aquaculture sites at different spatial and temporal resolutions. Earth Observation (EO)-based long-term monitoring offers unique insights into the complex interactions between aquaculture and surrounding ecosystems. However, most studies on the spatio-temporal development of aquaculture have been conducted at local or regional scales rather than continental ones (Duan et al., 2021; Duan et al., 2021; Stiller et al., 2019; Zhe et al., 2020; Zhe et al., 2020). Cloud cover is limiting the data collection with passive optical satellite sensors, particularly in tropical and subtropical coastal regions, where building a cloud-free dataset is difficult - even with EO missions like Landsat or Sentinel-2, which feature higher revisit frequencies and wider swath widths. Active radar sensors such as Sentinel-1, operating in the longer microwave range, overcome this limitation by being less influenced by atmospheric conditions and offering weather-independent imaging (Ottinger and Kuenzer, 2020). Advanced remote sensing methods, including machine learning methods, such as image segmentation, support vector machine, and neural networks, have been applied to extract aquaculture features. Image segmentation-based feature extraction (Fu et al., 2019; Zhang et al., 2020) have been applied to preprocessed satellite imagery data and integrated methodological approaches combining spectral, spatial, geometric, morphological, topographic, and topological features to separate aquaculture from other land cover types (Ottinger et al., 2022; Ottinger et al., 2017; Prasad et al., 2019; Sun et al., 2020; Tian et al., 2022; Wang et al., 2022; Xia et al., 2020). In addition to edge-oriented image segmentation methods (e.g., Laplace or Sobel operators, Canny Edge Algorithm (Canny, 1986)), thresholding is widely used for object recognition in digital image processing (Hay et al., 2003; Li and Lee, 1993; Liu et al., 2006). Recent studies have examined long-term dynamics of aquaculture ponds at single-pond level in China's Pearl River Delta and Yellow Rover Delta (Stiller et al., 2019). Non pond-specific approaches analyzing the spatiotemporal development of aquaculture areas with EO data focus on detecting agglomerations of larger pond areas (not at single pond level). Such studies have been conducted for Hainan Island (Fu et al., 2021), coastal China (Duan et al., 2021; Ren et al., 2019; Wang et al., 2023), Vietnam (Zhe et al., 2020), and Southeast Asia (Jiang et al., 2024; Luo et al., 2022; Zhang et al., 2023).

This paper introduces an innovative EO-based approach for monitoring the spatiotemporal development of land-based pond aquaculture in the coastal zone of Asia, focusing on a comprehensive cross-country analysis of long-term aquaculture dynamics. This was achieved through the use of high-resolution Earth Observation data, particularly Sentinel-1 and Sentinel-2, to derive a detailed reference dataset of pond aquaculture (Ottinger et al., 2022), complemented by an extensive analysis of the entire Landsat archive to assess water coverage of each pond object over time. For the first time, our study offers a pan-Asian, high-resolution analysis of pond aquaculture development patterns, overcoming the limitations of previous research that have focused on local or regional scales. While previous studies primarily focused on detecting pond areas at regional or national scales, our approach goes a step further by tracking the evolution of each individual pond over time. Using the computational power of Google's Earth Engine platform and analysis ready datasets, we efficiently processed large-scale, multi-decadal data, enabling detailed assessments of aquaculture dynamics. Our study goes beyond monitoring aquaculture status for the reference pond dataset by conducting spatial analyses of pond distribution patterns, as well as examining temporal changes in pond development at both national and sub-national levels. Additionally, we compared satellite-derived aquaculture pond areas with official statistics on pond production from FAO, enabling a validation of spatially explicit

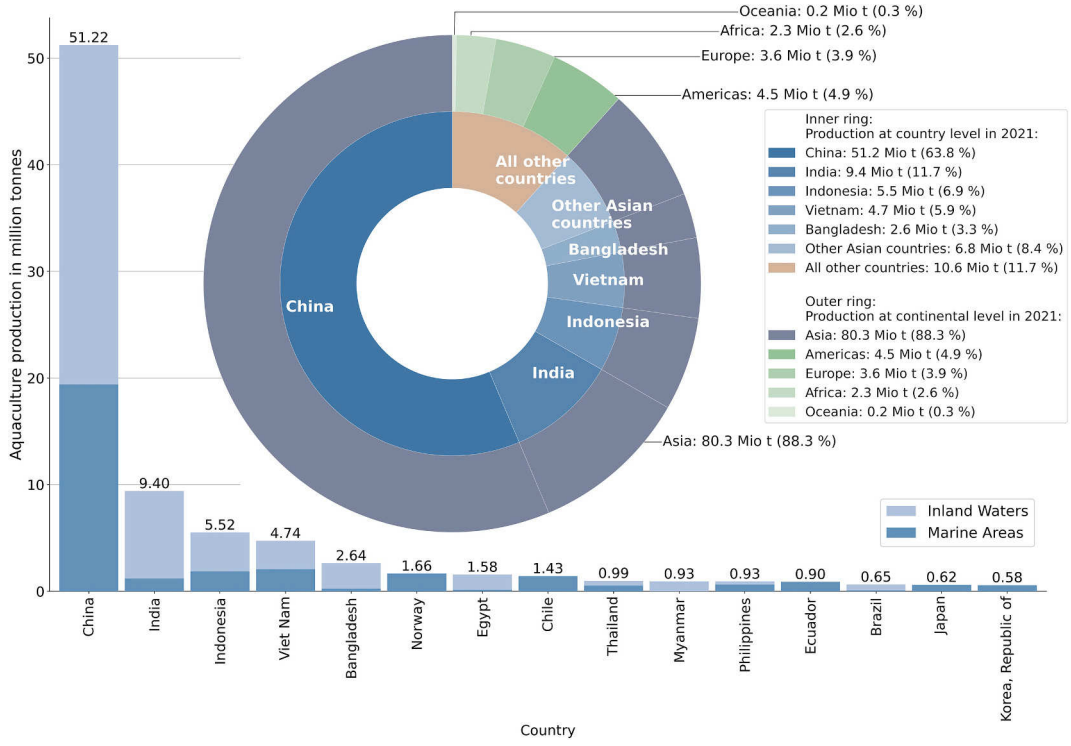

Fig. 1. Bar chart: Aquaculture production in inland waters and marine areas among Asian countries in 2021; Donut chart: Share of aquaculture production among continents and the top 5 global producers in 2021. Data source: FAO (2021). Figure updated and modified according to Ottinger et al. (2022).

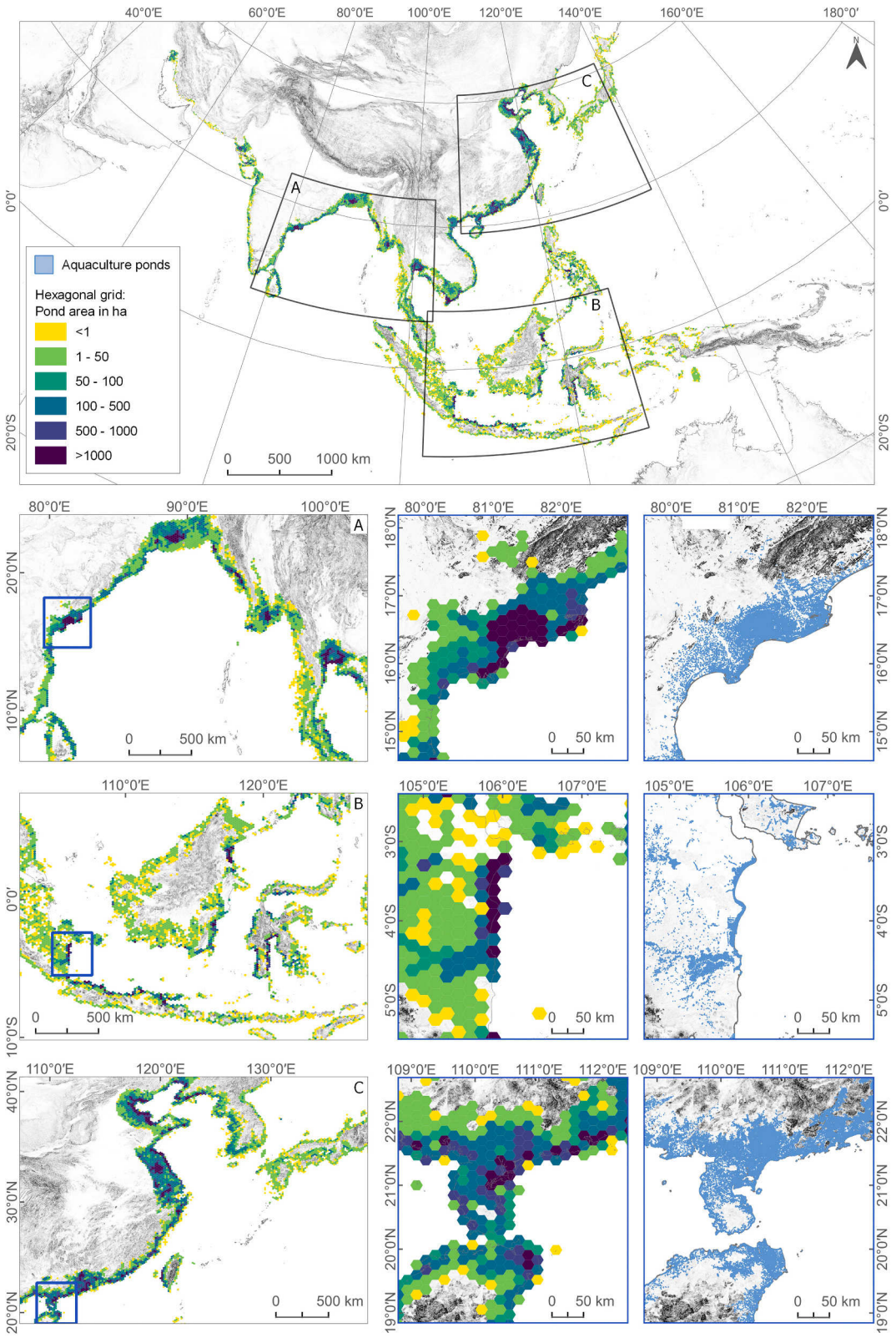

Fig. 2. Map of coastal aquaculture ponds in Asia. The pond dataset was derived from satellite-based Earth observation time series data (Sentinel-1 and Sentinel-2) for the year 2019. Data source: Ottinger et al. (2022).

aquaculture trends against reported aquaculture production data. This approach provides a unique, granular perspective on pond aquaculture development, offering insights into the local and regional trends across Asia. It also assesses the impact of local policies and environmental factors on pond development, providing valuable information for sustainable coastal aquaculture management. By understanding the historical and current status of individual ponds, decision-makers can develop targeted strategies for sustainable aquaculture practices, contributing to evidence-based management and ensuring long-term food security. The sub-national level analysis also allows for a more

nuanced understanding of regional disparities and potential areas, aiding for targeted interventions.

2. Study region

The investigated study region encompasses the coastal zone of Asia spanning South Asia, Southeast Asia, and East Asia, covering a total of 22 countries and a coastline that extends 300,000 km (as depicted in Table 1). To delineate the coastal zone of Asia (CZA) for this study, a calculation was performed by establishing a 200-km buffer both towards the land and the sea, originating from a detailed representation of Asia's coastline. With the aim of facilitating the efficient processing of annual water masks derived from satellite time series data across the entire Asian coastal zone, we defined and used coastal segments for further processing. Therefore, a total of 261 distinct coastal parcels (as illustrated in Fig. 4) - each spanning an interval of 200 km - were calculated as lateral segments along the coastline within a 200 km wide coastal buffer. Extending from Iran in the west to Western New Guinea in the southeast, and encompassing Japan in the northeast, the coastal zone is densely populated and has a cumulative population of more than 1.726 billion people (2015) within a 200 km distance from the coastline (European Commission, Joint Research Centre, 2015; see Table 1). This represents 41 % of the total population of the countries in this zone and accounts for 20 % of the global population. Along Asia's coast, the low-lying, flat-topography areas (including lagoons, estuaries, river deltas) facilitated the rapid expansion of pond aquaculture. Rapid socio-economic development, increased urbanization, and coast-ward migration (Neumann et al., 2015), however, dramatically changed the coastal regions in Asia during the last two decades. Land use changes were closely related to the expanding farming of crops (e.g., paddy rice), fish and shrimp, which are the main food source for millions of people. At both continental and national scales, significant variations in aquaculture production exist across different regions. The five leading aquaculture-producing nations collectively contribute over 80 % of the global output, with all located in Asia: China (51.2 million t), India (9.4 million t), Indonesia (5.5 million t), Vietnam (4.7 million t), and Bangladesh (2.6 million t) (FAO, 2023; see Table 1). Notably, in 2021, China's share in global aquaculture production exceeded half, accounting for 63 %, thereby underscoring its important role within the aquaculture food sector in recent times.

3. Data & methods

3.1. Data

3.1.1. Reference ponds

The reference pond areas for the spatio-temporal analysis of aquaculture development are based on an automatic multi-sensor approach for object-based extraction of land-based pond aquaculture which was developed by Ottinger et al. (2022). This approach generated the first comprehensive, continental-scale dataset of mapped pond aquaculture at the single objects level. The dataset was created for the year 2019 using space-borne image time series data acquired by the Sentinel-1 and Sentinel-2 missions, both integral parts of the Copernicus Earth Observation Program operated by the European Space Agency (ESA). The automatic extraction method applied for the entire Asian coastal zone utilized all accessible Sentinel-1 Ground Range Detected (GRD) and Sentinel-2 Surface Reflectance (SR) images for the same year. Utilizing the Digital Elevation Model (DEM) from the Shuttle Radar Topography Mission (SRTM), the initially identified polygons were refined by considering the relief they occupied; specifically, only those situated in flat and low-lying coastal areas were retained. Subsequently, these polygons were additionally filtered based on size and shape features to exclude other types of water bodies unrelated to aquaculture ponds. When compared to the very high-resolution optical imagery accessible on Google Earth, the mapping result for coastal ponds demonstrated an overall accuracy of 91.9 % (Ottinger et al., 2022). The final pond vector dataset from Ottinger et al. (2022) covers ponds across the entire coastal

Table 1
Overview of all countries to the study region sorted by aquaculture production (descending order).

Country	Number of reference ponds[a]	Reference ponds[a] area [ha]	Coastline length[b] [km]	Population in the coastal zone[c] [in Mio]	Aquaculture production (AP) in tonnes in 2021[d]	World rank by AP in 2021[d]
China[1]	1,432,575	1,153,618	34,362	429.65	51,221,122	1
Indonesia	383,805	269,251	97,680	250.32	9,403,000	2
India	345,116	224,548	13,166	386.57	5,515,227	3
Vietnam	662,390	151,486	6217	87.09	4,736,120	4
Bangladesh	167,346	71,524	2735	82.94	2,638,745	5
Thailand	260,713	140,990	8182	39.09	989,898	9
Myanmar	90,476	88,444	18,008	28.52	929,217	10
Philippines	86,991	91,581	34,541	96.78	928,821	11
Japan	48,594	14,279	30,725	121.38	621,580	14
Republic of Korea	13,434	15,550	14,930	48.4	581,995	15
Iran	19,209	10,495	5858	10.48	478,737	16
Cambodia	24,007	12,355	1430	10.91	347,350	19
Taiwan, Province of China	47,085	19,380	2863	23.06	274,500	23
Malaysia	30,543	17,168	12,465	29.73	238,082	25
Pakistan	29,326	23,684	4936	24.27	164,527	30
Dem. People's Rep. Korea	9037	9521	4896	23.71	77,560	43
Sri Lanka	11,089	15,428	3930	20.58	50,759	47
Singapore	–	–	490	5.44	5244	92
Brunei Darussalam	829	502	298	0.43	4768	98
China, Hong Kong SAR	1024	1356	1101	5.93	3909	101
Timor-Leste	224	68	803	1.17	391	142
ROI total	3,663,813	2,004,501	299,705	1726	79,211,550	

[1] including Macao SAR; ROI: Region of interest (ROI) refers to all Asian countries, which cover the coastal zone of Asia (CZA).
[a] Area (in ha) of reference pond aquaculture objects per country, source: Ottinger et al. (2022).
[b] Coastline length calculated from vector data on administrative areas from the GADM (GADM, 2012) dataset.
[c] GHS-POP R2015A-GHS population grid, derived from GPW4 (European Commission, Joint Research Centre, 2015).
[d] Aquaculture production (excluding photosynthetic active organisms such as seaweed) according to FAO Fishery and Aquaculture Statistics.

zone of Asia, as depicted in Figure 2. This dataset comprises a total of 3.6 million pond features from 22 countries (see Table 1). As no specific details were provided regarding the type of pond water, it was assumed that the reference ponds encompassed both freshwater and brackish water ponds.

3.1.2. Landsat satellite data

In this study, annual water masks were created using all available optical satellite images acquired by the Landsat fleet covering the entire Asian coastal zone. The Landsat program, a longstanding Earth observation initiative, comprises seven satellites jointly operated by the National Aeronautics and Space Administration (NASA) and the United States Geological Survey (USGS). These satellites capture multispectral optical data with a ground resolution of 30 m and operate on an approximate revisiting cycle of 16 days (see Table 2). The extensive and openly accessible Landsat archive containing multi-spectral time series data, provides valuable long-term Earth Observation monitoring capabilities for high-resolution and large-scale mapping of water dynamics and is therefore suitable to spatio-temporal development (status of water coverage) for pond aquaculture objects.

In our research, Landsat Surface Reflectance (SR) products from the Google Earth Engine (GEE) (Gorelick et al., 2017) were utilized. These are accessible in an analysis-ready format (ARD) and have been pre-processed applying radiometric calibration, orthorectification, and atmospheric calibration. For the scope of this study, Landsat SR images captured from January 1, 1984, to December 31, 2019, were selected to match with the temporal range corresponding to the reference ponds which were detected for the year 2019. Details about each sensor can be found in Table 2. The spatial and temporal coverage of Landsat scenes varies, with areas situated within overlapping zones between two or more Landsat footprints undergoing more frequent imaging than regions outside these overlapping zones. Images from the late 1980s and early 1990s are less prevalent during the observed time span. Since this study generated annual water masks, the count of observations per year was a focal point. To also address the Landsat 7 striping issue caused by the Scan Line Corrector (SLC) failure, we utilized temporal compositing by aggregating multiple images from different dates into annual composites (e.g. median, see section 3.2.1), effectively filling gaps and reducing the striping effect, ensuring reliable and accurate data for our analysis. Fig. 3 illustrates the total observation counts within the complete Landsat archive-based image time series stack at the pixel level from 1984 to 2019. The red areas in Fig. 3 represent locations where the number of images is below 100. However, these red areas are primarily located over the sea and did not affect the analysis, which focused on land-based pond objects along the coastal zone. The vast majority of the land areas have more than 250 images for the study period, which is sufficient to generate annual water masks and conduct a thorough analysis of the water status for the land-based reference pond objects.

3.1.3. Administrative data

The spatial and temporal evolution of pond aquaculture will be presented across various administrative levels, spanning from the national to the district level. The administrative data has been downloaded from the Database of Global Administrative Areas (GADM) (GADM, 2012). For the 22 countries (see Table 1) the number of districts containing reference ponds is 92 for China, 390 for Indonesia, 121 for India, 502 for Vietnam, 40 for Bangladesh, 362 for Thailand, 31 for Myanmar, 1092 for Philippines, 1121 for Japan, 147 for South Korea, 26 for Iran, 118 for Cambodia, 21 for Taiwan, 123 for Malaysia, 6 for Pakistan, 111 for North Korea, 194 for Sri Lanka, 29 for Brunei, 12 for Hong Kong SAR, and 27 for Timor-Leste.

3.1.4. National statistical data on aquaculture production

The Food and Agriculture Organization of the United Nations (FAO) member countries voluntarily report their fisheries and aquaculture data to the organization, and FAO then compiles and analyzes this information to produce global, regional, and country-specific reports on aquaculture. These data are freely accessible through FAO's FishStatJ software, which provides statistical databases on fisheries and aquaculture time series from 1950 onwards (FAO, 2023). We downloaded the data set 'Global aquaculture production quantity (1950 - 2021)' and compared it with the water coverage time series of the mapped pond aquaculture area in the discussion section. To align with the objectives of this research, we refined the FAO dataset to include production quantities specifically for fish, crustaceans, and mollusks (excluding aquatic photosynthetic organisms, such as sea weed) cultivated in fresh and brackish water across all 22 coastal Asian countries. This refinement was achieved by applying filters based on criteria such as country, culture system, and species. The resultant subset of the dataset specifically represents the production quantity of fish, crustaceans, and mollusks from freshwater and brackish water culture in all 22 coastal Asian countries, forming a key focus in this study.

3.2. Methods

For all the reference ponds detected and extracted using Sentinel-1 and Sentinel-2 data for the year 2019, we established a framework (see Fig. 4) to determine the yearly aquaculture status for each individual pond. This determination was based on annual water masks derived from the multi-decadal time series data provided by the Landsat archive spanning the period from 1984 to 2019. A receiver operating characteristic (ROC) test was used to delineate detailed water masks for overlaying with the pond reference dataset. This method allows us to assess aquaculture pond presence over time for the reference pond dataset by checking how these water masks align with the reference dataset, assuming that active ponds are covered by water during the Landsat observation period.

3.2.1. Water mask generation

Water masks were generated using a unique threshold applied to an annually derived water index image, which was processed based on Landsat time series data for each coastal parcel. A total of 261 water mask files were created, corresponding to the 261 coastal parcels outlined in Fig. 3. Each water mask file contains 35 bands, with each band representing the annual water mask for a given year from 1985 to 2019. To identify the optimal combination of water index and reducer for

Table 2
Details on the Landsat missions and spectral bands relevant for the study.

Satellite	Instrument	Operational from-to	Revisit time	Spatial resolution*	Swath width	Bands	Band width (μm)
Landsat 4	Thematic Mapper (TM)	1982–1993	16 d	30 m	185 km		L4/L5/L7 | L8
Landsat 5	Thematic Mapper (TM)	1984–2011	16 d	30 m	185 km	Blue	0.45–0.52 | 0.45–0.51
Landsat 7	Enhanced Thematic Mapper (ETM^+)	1999	16 d	30 m	185 km	Green	0.52–0.60 | 0.53–0.59
						Red	0.62–0.69 | 0.64–0.67
Landsat 8	Operational Land Imager (OLI)	2013	16 d	30 m	185 km	Nir	0.77–0.90 | 0.85–0.88
						Swir1	1.55–1.75 | 1.57–1.65
						Swir2	2.08–2.35 | 2.11–2.29

* Spatial resolution for the short-wave channels; TM has an additional thermal infrared (TIR) band with a spatial resolution, the ETM^+ is equipped with a 15 m Panchromatic (PAN) band and 60 m TIR band, and OLI has a 15 m PAN band.

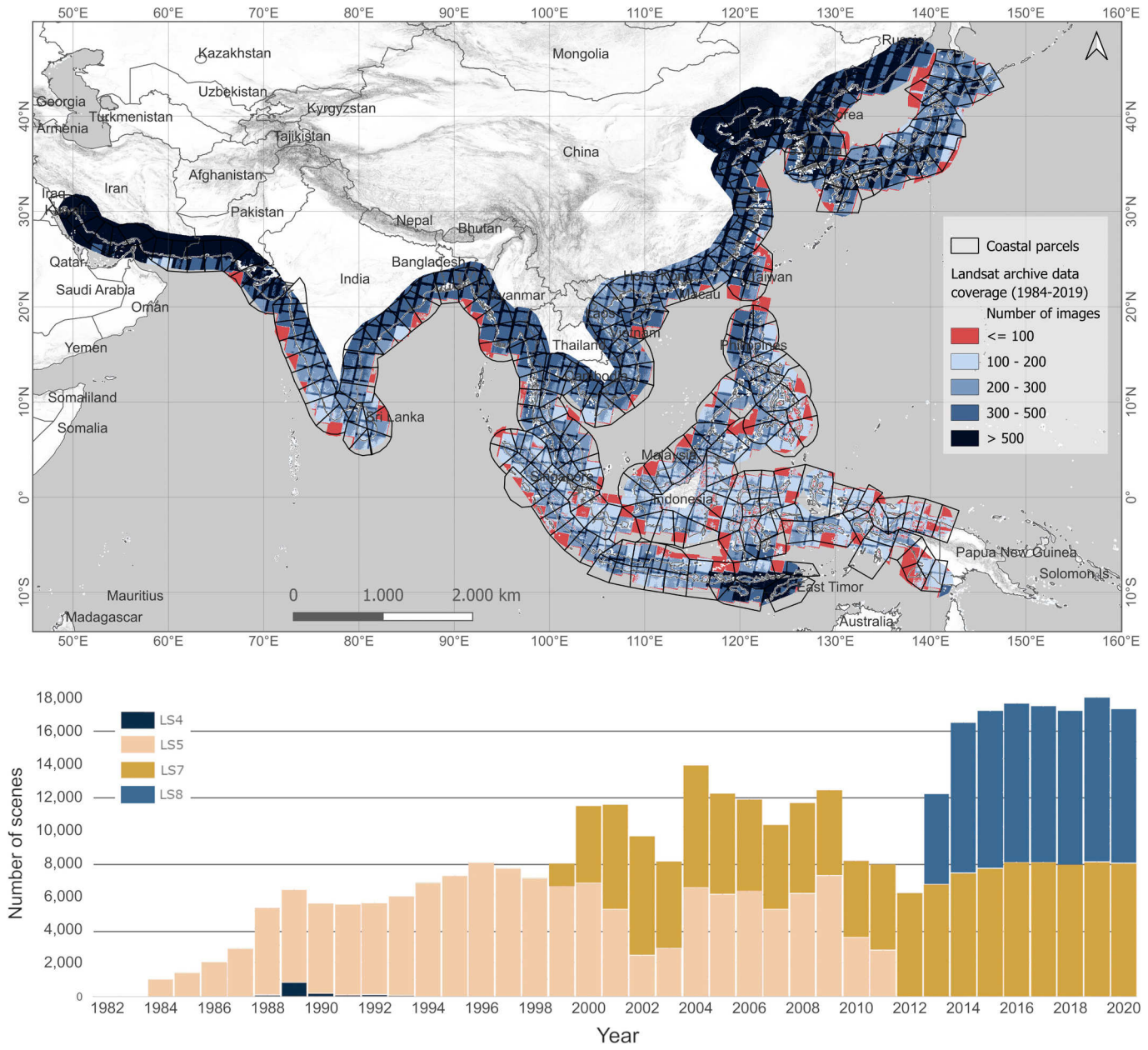

Fig. 3. Top: Map of the study region, including a total of 261 coastline parcels that encompass a coastline of ~200 km in length. Bottom: Data coverage of Landsat Archive (LS4-LS8) data from 1984 to 2019 for the coastal zone of Asia.

accurately extracting water bodies and depicting the pond water coverage status on an annual basis for a long-term time series (based on Landsat data), a receiver operating characteristic curve analysis, referred to as ROC test hereafter, was conducted. Eight coastal test sites distributed along the coastal zone of Asia were utilized for this analysis (see Fig. 5). Initially, all Landsat images captured in 2019 were selected and preprocessed to remove clouds and cloud shadows. Each cloud-free image was then used to calculate four distinct water indices for the ROC test: Normalized Difference Water Index (NDWI) (McFeeters, 1996), Modified Normalized Difference Water Index (MNDWI) (Xu, 2006), Automated Water Extraction Index (AWEI) (Feyisa et al., 2014) and the water index proposed by Fisher et al. (2016), referred to as WIFI in this study. The equations for calculating these indices can be found in Table 3.

In a next step, all images were aggregated at the pixel-level using a reducer. To account for potential outliers during the ROC test, the median operator was selected as the reducer method. To enhance the detection of ponds intermittently covered by water throughout the year, the 95th percentile was also employed as a secondary reducer for the test. The output of this step consisted of images representing the median values of NDWI, MNDWI, AWEI, WIFI, as well as the 95th percentile values of NDWI, MNDWI, AWEI, and WIFI for the year 2019. For each of these images, Otsu's method was applied to establish an initial threshold for the extraction of water bodies. Otsu's method (Otsu, 1979), a threshold selection technique, distinguishes objects based on the histogram of pixel values within an image. It performs optimally when the histogram exhibits two distinct peaks, representing objects and the background, with a significant valley between them. To ensure a bimodal distribution (two peaks) of DN values in each histogram, the water index images were processed at a parcel-level basis (refer to coastal parcels in Fig. 3). Each parcel consisted of two 200 km buffer areas, one extending inland and the other towards the sea (Ottinger et al., 2022), ensuring an even distribution of land and water areas. From each reduced image, multiple water masks were generated by

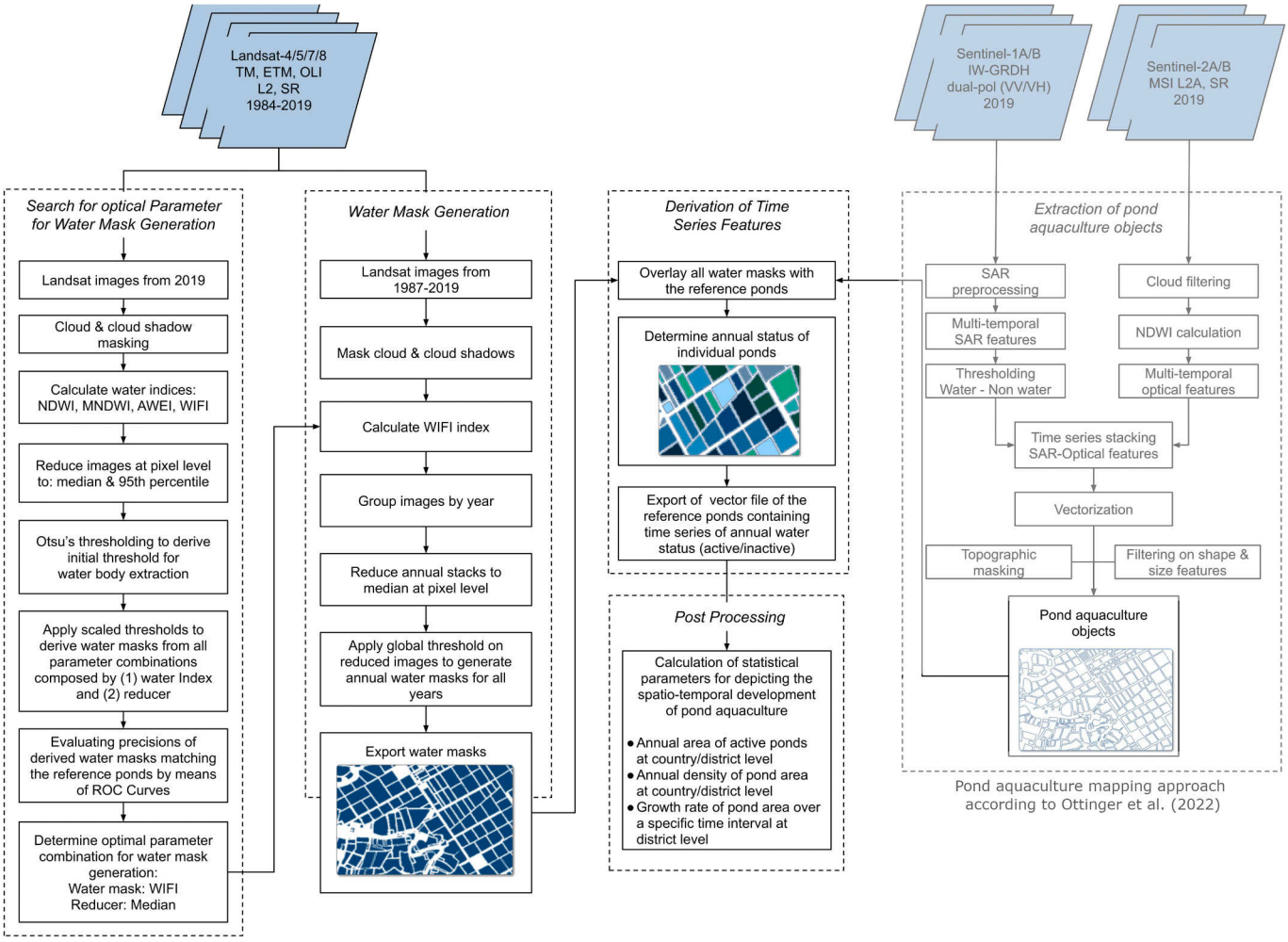

Fig. 4. Processing workflow. Left part (columns 1–2-3): Automatically derived water masks were computed to determine the aquaculture status (active/non-active/cloud covered) for each pond object for the complete pond aquaculture dataset for the year 2019. This dataset was obtained through the multi-sensor (Sentinel-1 and Sentinel-2) approach by Ottinger et al. (2022).

applying the automatically derived Otsu's threshold. The entire processing workflow for this task was conducted using the Google Earth Engine (GEE) Python API (Gorelick et al., 2017) running on a docker environment on a local Linux server.

For the ROC test, a total of 64 water masks were generated for the test sites through a combination of the median and 95th percentile reducer, water index, and a global threshold (8 combinations for each of the 8 test sites resulted in a total of 64 water masks to be used for the ROC test). These water masks were used as input at each test site, spanning every year from 1984 to 2019 and covering the entire study area (coastal zone of Asia). All images underwent preprocessing steps, including the removal of cloud and cloud shadows, and NDWI, MNDWI, AWEI, and WIFI bands were computed and added to each image. Subsequently, the images were organized into image stacks for each year, and these annual stacks were reduced to new images representing the annual median and 95th percentile for all four water indices. OTSU's threshold was then computed and applied to each reduced image to delineate water bodies from the land surface. Water pixels were assigned the integer value 1, land pixels were assigned integer value 0 and no data pixels were assigned the integer value 2.

For accurate analysis, the water mask must closely match the actual ground truth ponds. However, the reference ponds were not used as ground truth for the ROC test because the reference ponds dataset does not include other types of water bodies, such as rivers or lakes, as illustrated in Fig. 5. Using the EO derived reference pond dataset as ground truth could lead to an overestimation of the false positive rate in the ROC analysis. Therefore, the ground truth ponds were manually delineated based on very high-resolution images from Google Satellite, ensuring a more accurate representation of pond boundaries (Fig. 6A-6G).

The ROC curve serves as a method for quantifying diagnostic accuracy, with the true positive rate (TPR) and false positive rate (FPR) represented on the Y and X axes, respectively. As the ROC curve approaches the left and top boundaries of the graph (see Fig. 6), it indicates an increasing proximity to perfect accuracy. In this study, individual parameter pairs were plotted on the ROC graph, where a point's proximity to the upper-left boundary indicates a higher precision in matching the derived water mask to the ground truth water body layer. To assess this alignment, each water mask was overlaid onto the ground truth water body layer, and points were sampled at 30-m intervals. A sampled point was classified as a true positive (TP) or true negative (TN) if it indicated "water" or "non-water" on both layers. False positives (FP) were identified when a sample was labeled as "water" on the derived water mask but as "non-water" on the ground truth pond layer, while false negatives (FN) occurred when a sample was labeled as "non-water" on the derived water mask but should have been identified as "water". The ROC curves plot the true positive rate (TPR) versus the false positive rate (FPR) for different parameter combinations. TPR is the proportion of reference water pixels that are correctly classified (or producers' accuracy), and FPR is the proportion of reference non-water pixels

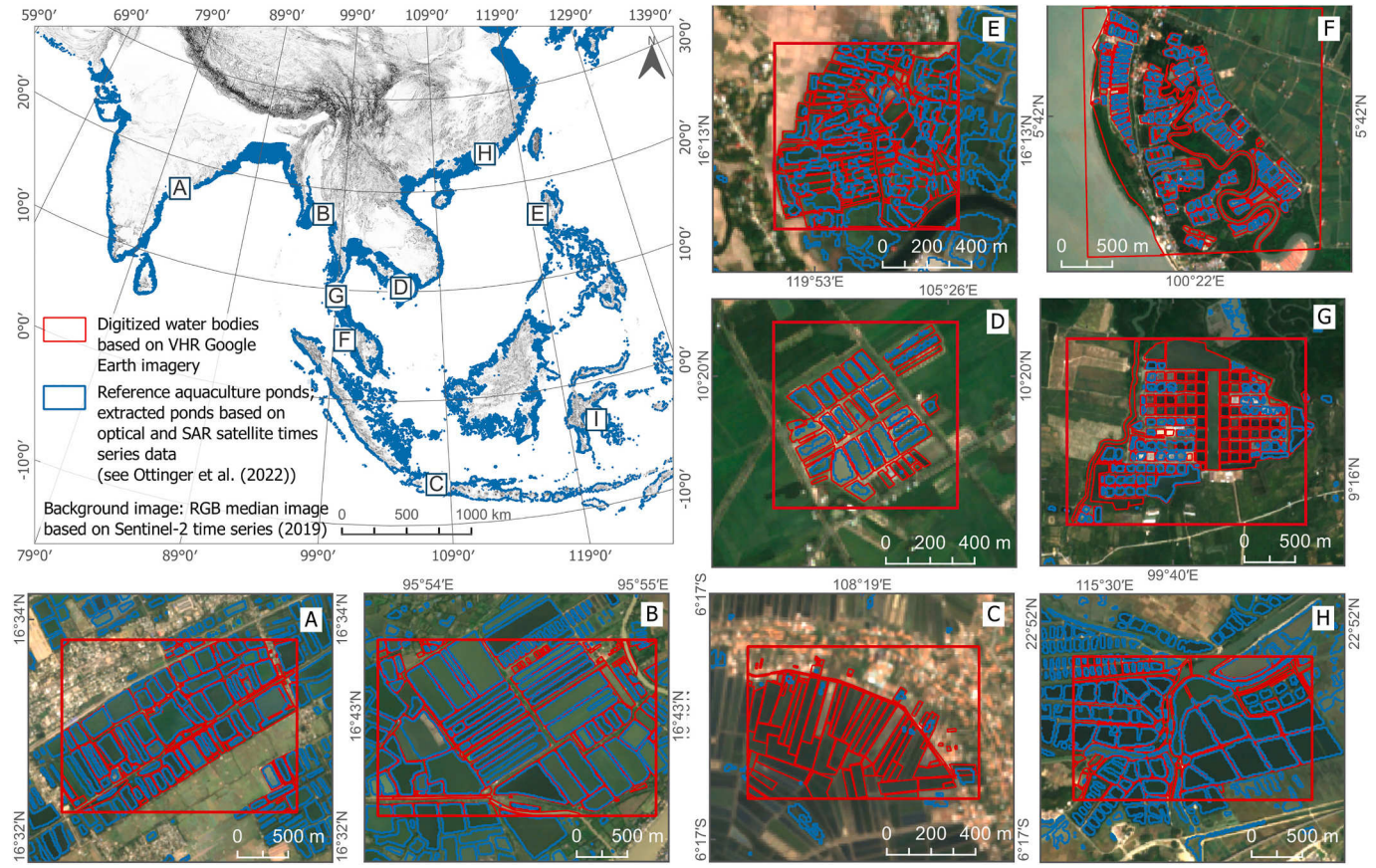

Fig. 5. Map showing the locations of all test sites along the coastal zone of Asia: A in India, B in Myanmar, C in Indonesia (Java), D in Vietnam, E in Philippines, F in Malaysia, G in Thailand, H in China, I in Indonesia (Saluwesi)) were used to select to generate water masks and test the performance of different water indices (see Table 2) and reducers. Red polygons: manually digitized water bodies on base images from VHR Google Earth satellite imagery; blue polygons: reference aquaculture ponds for the year 2019 as described in Ottinger et al. (2022). (For interpretation of the references to colour in this figure legend, the reader is referred to the web version of this article.)

wrongly classified as water. From the ROC graph, it is evident that AWEI and WIFI were more effective water indices than NDWI or MNDWI. Regarding the reducer, we see that the median performed better than the 95th percentile. The relationship between the thresholds associated with "median AWEI" and "median WIFI" and the distance from their points on the ROC curve to the upper-left boundary indicates that the WIFI median has the best combination of water index and reducer. For this reason, we selected the WIFI median for the subsequent generation of annual water mask based on Landsat time series data. These masks served as the data basis for determining the water coverage status for each individual pond polygon (active pond/non-active pond).

3.2.2. Pond status determination

By overlaying the annual water masks onto the reference ponds, the status of individual ponds for each year was determined based on the predominant pixel values covering each pond in the water masks. For example, if a pond covers a total of 2 × 2 pixels in the water mask, with two pixels having value of 1, one pixel with a value of 0, and one pixel with a value of 2 for a given year, it was considered active for that year. The determination process was carried out using the zonal statistics (zonal_stats) function from the rasterstats package in Python.

Table 3
Tested water indices. (B) for bands of Landsat images.

Index	Equation
NDWI (McFeeters, 1996)	*(Bgreen – Bnir) / (Bgreen + Bnir)*
MNDWI (Xu, 2006)	*(Bgreen - Bswir1) / (Bgreen + Bswir1)*
AWEI (Feyisa et al., 2014)	*Bblue + 2:5 × Bgreen - 1:5 × (Bnir + Bswir1) - 0:25 × Bswir2*
WIFI (Fisher et al., 2016)	*1:7204 + 171 × Bgreen + 3 × Bred - 70 × Bnir - 45 × Bswir1–71 × Bswir2*

3.2.3. Regionally aggregated statistics

Following this, the time series of pond status for each pond and year were summarized at province- and district-level for each country to facilitate statistical analyses on administrative units. The parameters computed in this study to illustrate the pond aquaculture development over time and space include:

(1) Annual area of active ponds (A) accumulated at the country level
(2) Annual density of pond area (ρponds) accumulated at the district level

$$\rho ponds = \frac{A\ in\ District}{ADistrict} \times 100\%$$

(3) Annual growth rate of pond area (R) accumulated at the district level (y for year, Y for the 1-year interval)

$$R1Y = \frac{A_{y+1} - A_y}{A_y} \times 100\%$$

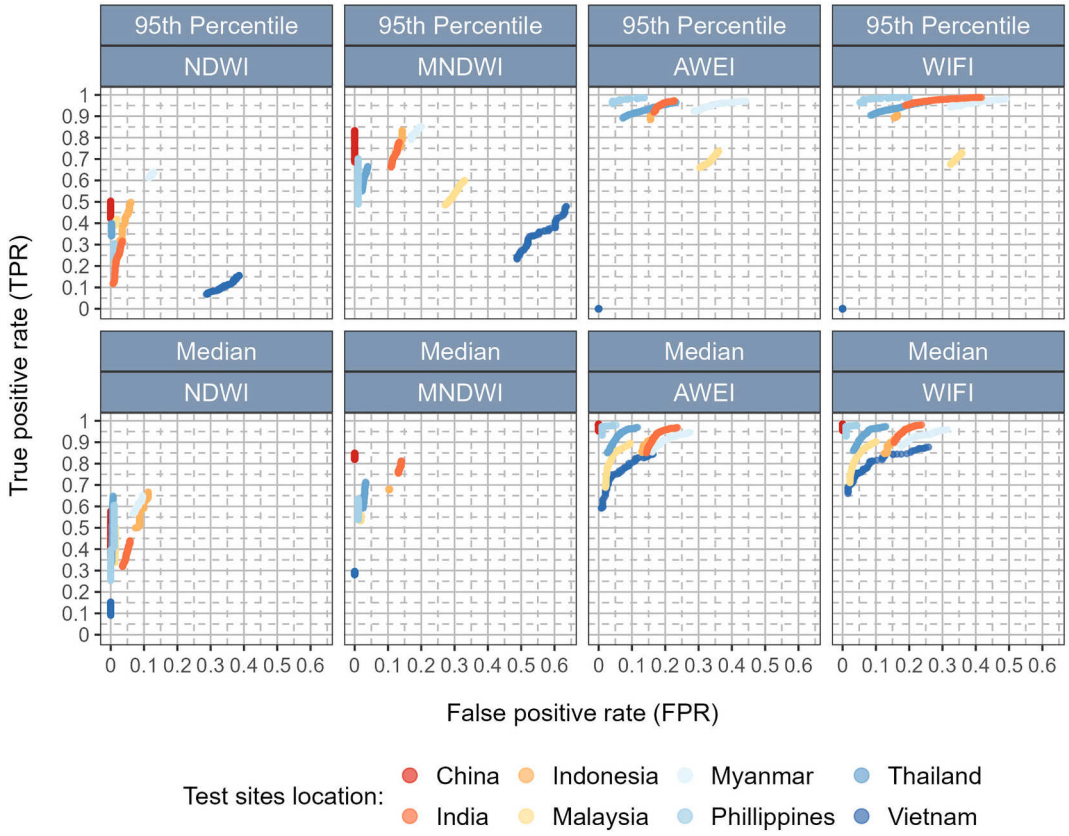

Fig. 6. ROC curves for different parameter combinations for all test sites.

(4) Average annual growth rates of pond area for a five-year interval (1986–2019) and ten-year interval (1991–2019) accumulated at the district level (T for time period, head for the first year of the period, tail for the last year of the period)

$$R\ 5Y \mid 10Y = \frac{A_{y+1} - A_y}{A_y} \times 100\%$$

In cases where a pond predominantly covered pixels with a value of 2 for a specific year, it was classified as "no data" for that year. It was found that the years in the mid-late 1980s and early 1990s exhibit larger data gaps (see Fig. 7). In total the overall share of no data pixels for all countries and years accounted for 2.37 %.

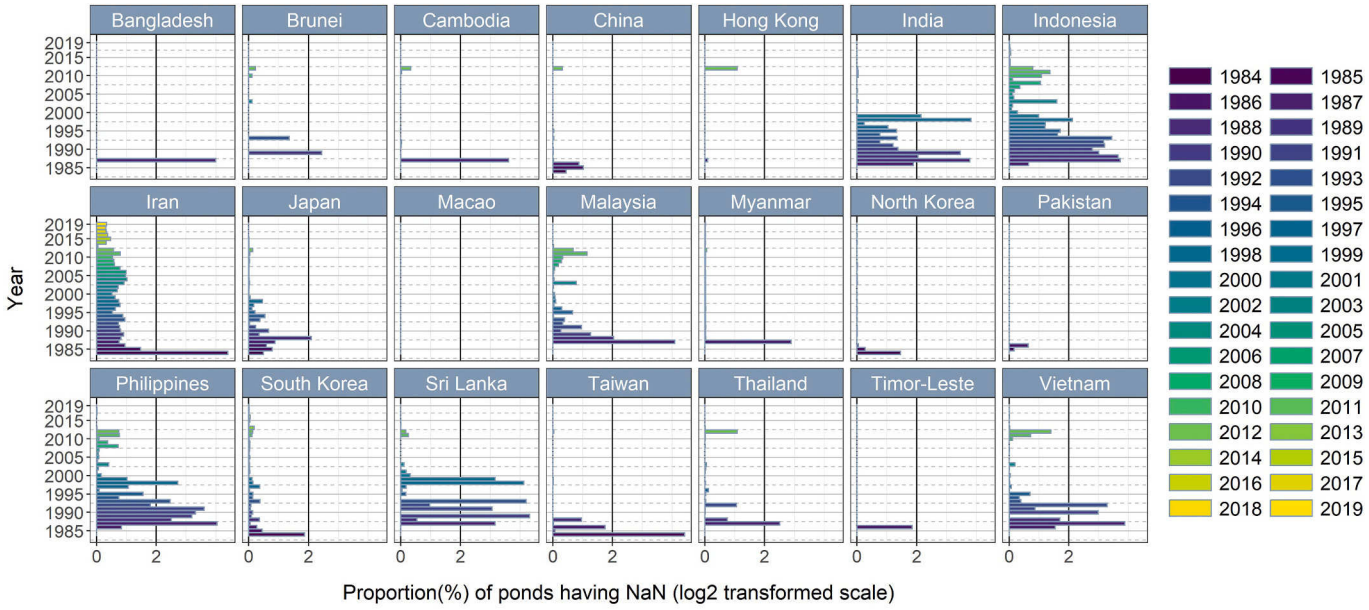

Fig. 7. Bar plot showing the proportion of ponds for which Landsat data was not available (NaN values).

3.2.4. Accuracy assessment

The accuracy of the generated water masks was evaluated by analyzing the percentage of reference ponds identified as active in the 2019 water masks. The calculation was performed as follows:

$$Accuracy = \frac{Detected\ active\ ponds\ of\ 2019}{Reference\ ponds} \times 100\% \quad (1)$$

4. Results

The accuracy assessment revealed that the overall accuracy of derived pond status of 2019 matching the reference ponds was 83.1 %. The overall accuracy for the top five aquaculture producing countries China, Indonesia, India, Vietnam, and Thailand was 76.9 %, 88.6 %, 81.5 %, 94.4 % and 89.2 % respectively.

4.1. Overall development pattern of pond aquaculture in Asia

The annual derivation of the aquaculture area status for individual aquaculture objects provides valuable information about the extent of these areas and reveals trends over time. With our approach, multi-temporal dynamics of pond aquaculture at the single-pond level were derived for the coverage of complete Asia using multispectral satellite time series provided by complete Landsat archive with a 30 m spatial resolution. Examining the period from the 1980s to 2019, it is evident that Asia has experienced substantial expansion in pond aquaculture areas across its coastal regions. As illustrated in Fig. 8, the reference ponds covered over 19,000 km^2 of land surfaces in 2019, while back in 1988 the total area accounted for about 6500 km^2. This rapid expansion observed over the three decades refers to a more than three-fold increase in total area. Among the examined countries, China utilizes by far the largest land area for pond aquaculture, followed by Indonesia, India, Vietnam and Thailand. From the reference ponds identified as active in 1990, 42.4 % (3803 km^2) were located in China, 14.4 % in India (1290 km^2), 8.5 % in Indonesia (757 km^2), 7.5 % in Vietnam (676 km^2), 7.0% in Thailand (630 km^2) and the remaining 20.1 % distributed across the other 17 countries. From the reference ponds identified as active in 2019 (see Fig. 8), 40.6 % (7856 km^2) were located in China, 13 % in Indonesia (2661 km^2), 11.2 % in India (2176 km^2), 7.7 % in Vietnam (1492 km^2), 7.2 % in Thailand (1387 km^2) and the remaining 19.6 % distributed across Philippines, Myanmar, Bangladesh, Pakistan, Taiwan, Malaysia, South Korea, Sri Lanka, Japan, Cambodia, Iran, North Korea, Hong Kong, Brunei, Macao and Timor-Leste.

In Asia, the overall aquaculture production has reached 80.3 million tonnes, constituting 88.3 % of the global aquaculture output (FAO, 2023). A significant trend in freshwater aquaculture growth has been driven by the widespread development of value chains across countries in South and Southeast Asia over the past decades, for example in Andra Pradesh in India (Belton et al., 2017), Bangladesh, Myanmar, Thailand (Belton and Little, 2008) and Vietnam (Loc et al., 2010). The expansion in freshwater aquaculture across Asia can be attributed primarily to increasing demand of aquaculture products while at the same time declining wild inland fisheries, which were once crucial for rural livelihoods and food security (Naylor et al., 2021).

Utilizing our EO-based pond aquaculture dynamics dataset, we have generated a map (see Fig. 9) that shows the spatio-temporal evolution of pond aquaculture at 5-year intervals. Fig. 9G, Fig. 9H and Fig. 9I highlight a distinct trend where the expansion of pond aquaculture areas is progressing inland wards - a pattern observed in various coastal regions. Since the initial development of aquaculture typically occurred near shorelines, the subsequent construction of newer ponds tends to take place in the available spaces situated behind the pre-existing ponds. This inland-ward driven spatial shift in aquaculture development reflects a dynamic development over time, contributing to the broader understanding of the aquaculture landscape and its evolving footprint. Concerning the spatial expansion of aquaculture ponds, an analysis of regional disparities was conducted by assessing the proportion of the total area covered by active reference ponds within specific distance ranges from the coastline. This analysis relies on the final vector dataset, incorporating administrative unit information from GADM (GADM, 2012), along with calculated coastline distances for each reference pond. From this dataset, we aggregated the annual area of active reference ponds within distinct coastline distance ranges. It can be observed that pond aquaculture exhibits a tendency to extend towards inland areas in Thailand, Myanmar, and Cambodia. The trend of inland-ward driven expansion is also evident for China, Bangladesh, and Pakistan, whereas this phenomenon is comparatively insignificant in Vietnam and India, and scarcely noticeable in Malaysia and Indonesia (refer to Fig. 10). However, certain considerations must be taken into account in this context. For example, the significant percentage of aquaculture ponds in Cambodia located at distances greater than 100 km (Fig. 10, categorized in yellow) can be attributed to the high concentration of Cambodia's main aquaculture production around Lake Tonle Sap - the largest freshwater lake in Southeast Asia. Moreover, it is also noticeable that the pond aquaculture tended to expand towards

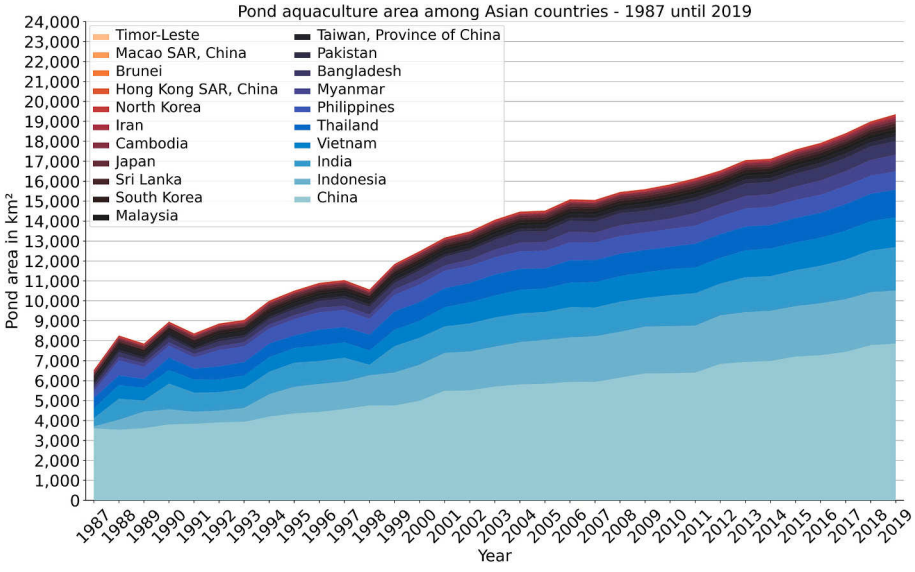

Fig. 8. Stacked area plot of the summarized areas (km^2) of active aquaculture ponds for each country during the investigated time period.

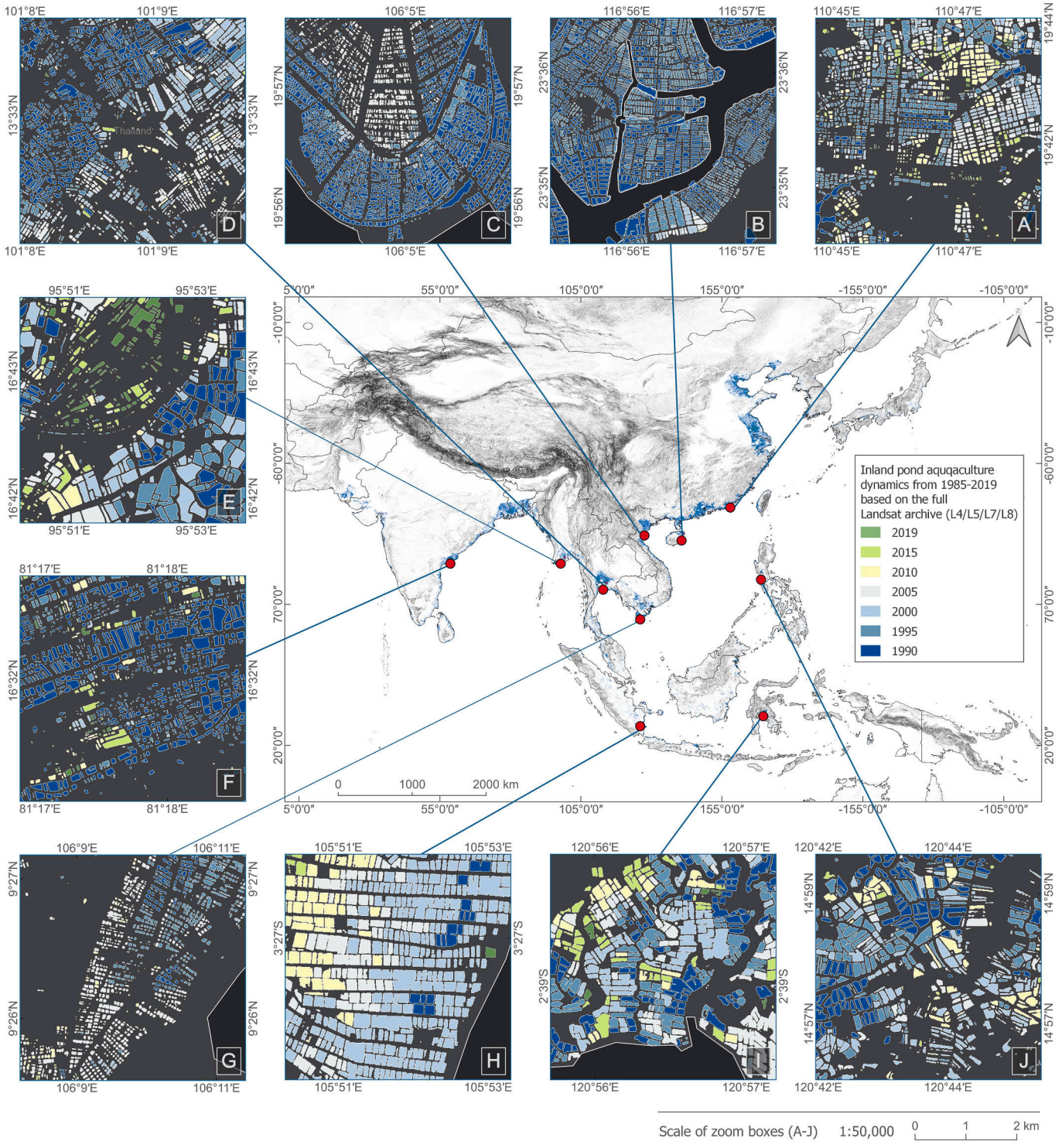

Fig. 9. Map with detailed zoom views on hotspot aquaculture regions showing the Landsat-derived active aquaculture status at pond polygon level from 1985 to 2019.

inland areas in China, Thailand, Myanmar, and Cambodia, while this phenomenon was insignificant in Vietnam and India and barely perceptible in Malaysia (Fig. 10).

4.2. Spatio-temporal development patterns of pond aquaculture in selected Asian countries

During the methodical implementation, the data set on aquaculture dynamics was joined with other vector files (i.e. distance to coastline, administrative units, SRTM DEM derived height and slope information), so that each individual aquaculture object contains various meta-information. This comprehensive integration ensures that each individual aquaculture object contains various meta-information, enabling country-specific aggregations across different administrative areas. The aim is to identify country-specific development patterns and describe how these patterns differ from those in other countries. Fig. 11 provides insights into the temporal changes in active reference ponds from 1987 to 2019. The left column presents the area of active reference ponds

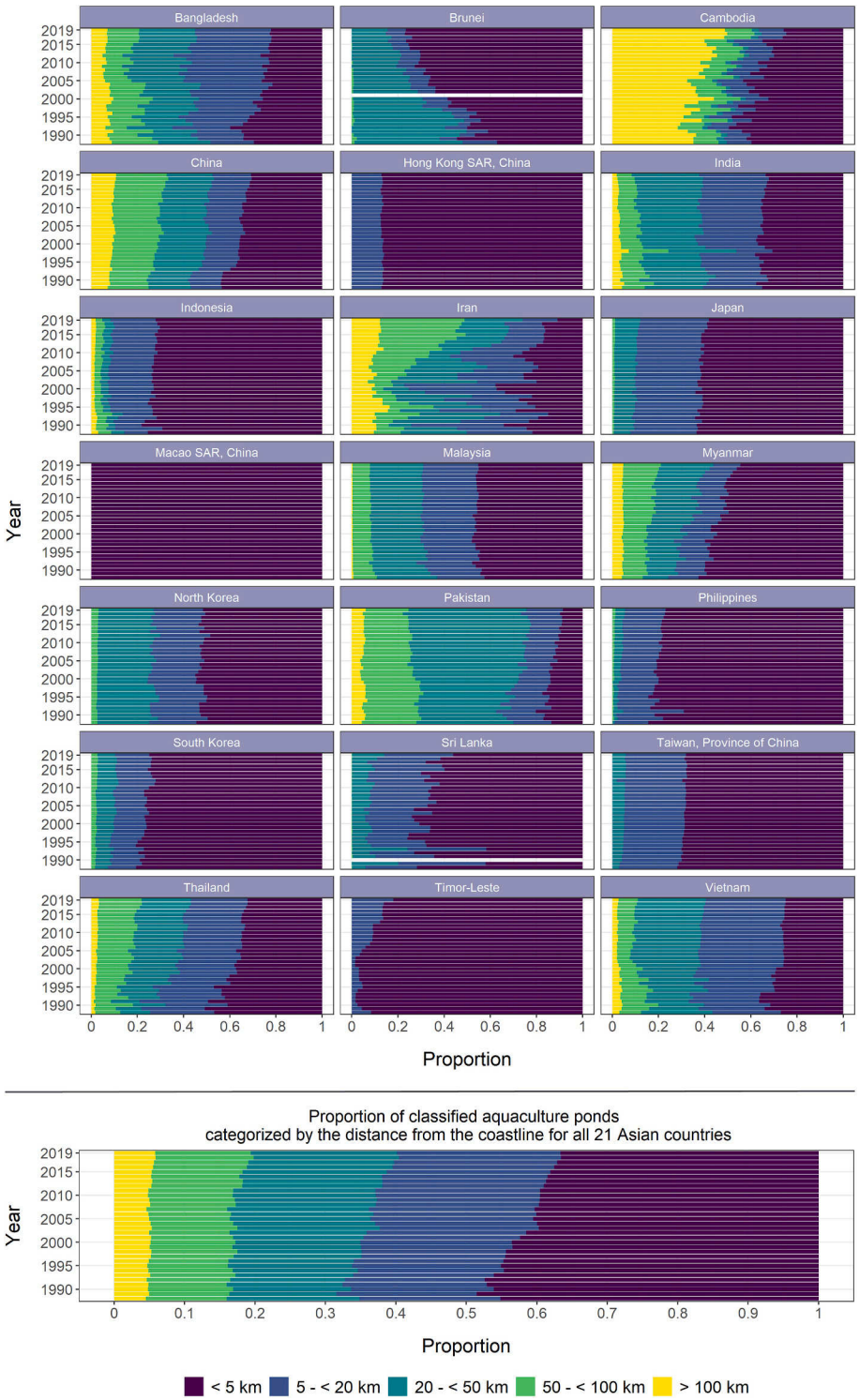

Fig. 10. Proportion of the reference ponds categorized by the distance from coastline for each year and country (plots in the top) and summarized for all countries (bottom).

from 1987 to 2019 (blue bar charts), while the right column shows the percentage difference between the area or number of active reference ponds for each year and the area or number of all reference ponds in the base year 2019 (line chart). Analyzing the spatio-temporal variabilities of growth of active reference ponds among the Asian countries it is evident that the growth was not evenly distributed. In Japan, South Korea, and the Philippines the increases of active reference pond area within the 1990s, 2000s, and 2010s is very low. However, in China, India, Indonesia, Thailand and Vietnam, reference aquaculture pond area increased significantly in the 1990s, 2000s and 2010s. While both India and Indonesia have experienced significant growth at a steady rate, Indonesia has generally grown at a faster rate. In India and the Philippines, the growth of active reference pond area has been more uneven, with significant fluctuations during the 1990s (see Fig. 11).

In the following section, we present a more comprehensive analysis of the five leading aquaculture producers in Asia:

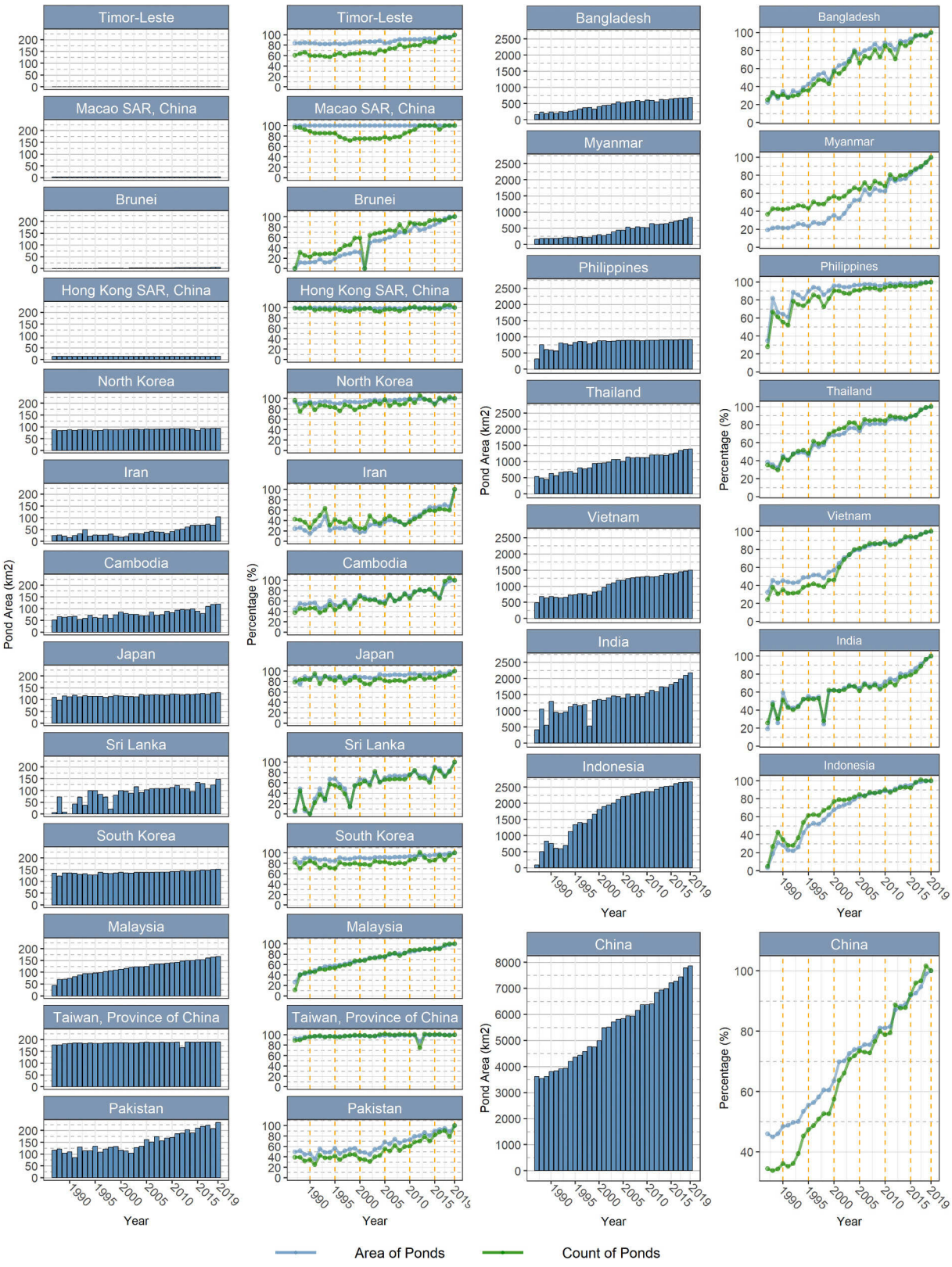

Fig. 11. First and third column: Yearly extent of active reference ponds by country; Second and fourth column: Percentage difference between each year's area or count of the active reference ponds and the area or count of all reference ponds (100 %) by country.

China: The analysis of temporal changes of reference ponds for China reveals a relative steady increase, with the total number and total area of reference aquaculture ponds nearly doubling from the 1990s to 2019. The total area of active reference ponds increased from around 3800 km^2 in 1990 to 5000 km^2 in 2000, 6300 km^2 in 2010 to 7850 km^2 in 2019.

India: In 2019, around 2170 km^2 of land surfaces were occupied by the reference ponds in India, with approximately half established in

1990 (1290 km^2). From late 1980s to 2000, the farmed area increased rapidly to 1800 km^2, despite some fluctuations, reaching 68 % of the 2019 size. Continuous growth occurred from 2000 to 2019, with acceleration in the last decade.

Indonesia: Approximately 2660 km^2 of land surfaces were utilized for pond aquaculture in 2019, with less than 30 % of the reference ponds established in 1990 (750 km^2). The cultivated area underwent rapid expansion from the early 1990s to mid-2000s. In terms of count, approximately 50 % of the reference ponds were already operational in 1988. Notably, from 2002 to 2004 and in 2011, the cultivated area increased more rapidly than the count of ponds, suggesting that more large-area ponds were likely constructed during those years.

Vietnam: An estimated 1510 km^2 of land surfaces were covered by the reference ponds in 2019, with approximately 65 % of this area existing in 1988. Pond area remained relatively stable in the early 1990s, followed by a thriving phase of significant expansion until 1999, reaching 75 % of the size observed in 2019. In the 2000s, the pond area expanded by approximately 20 % of the 2019 size. Subsequently, continuous growth without significant fluctuations occurred from the 2000s to 2019.

Thailand: The reference ponds encompassed approximately 1400 km^2 of land surfaces in 2019, with around 40 % being active in 1988. Before 2000, the cultivated area exhibited frequent abrupt fluctuations but consistently experienced substantial increases at high rates. Both the area and the count of reference ponds expanded, averaging 20 % of the 2019 size in a 5-year interval, reaching 80 % by the end of the 1990s. Post-2000, the expansion tended to slow down, taking an average of ten years to increase by 10 %, and the fluctuations appeared to become more subdued.

Among the observed regions, the coastal districts along the eastern coast of the Malay Peninsula in Thailand, the coastal area in Thailand close to Cambodia, and the Irrawaddy Delta in Myanmar appeared to be the arising hot spots of pond aquaculture production.

4.3. Aggregated pond aquaculture area growth rates

To explore spatio-temporal changes of pond area in administrative units, additional analyses was conducted using the density of the active reference pond area to evaluate land use intensity in pond aquaculture production. Concurrently, the growth rate of the area was employed as an indicator of the expansion pace in pond aquaculture. In our analysis of the 5-year average annual growth rates of the area of active reference ponds at the country level (Fig. 12), we find that growth rates tend to cluster within the range of 0 % to 10 %. Examining the annual growth rates at the district level (Fig. 13), we observe that growth rates generally remain between 0 % and 10 %, indicating a trend towards gradual expansion of pond farming area across more districts, as opposed to extensive expansions or contractions. This analysis demonstrates a

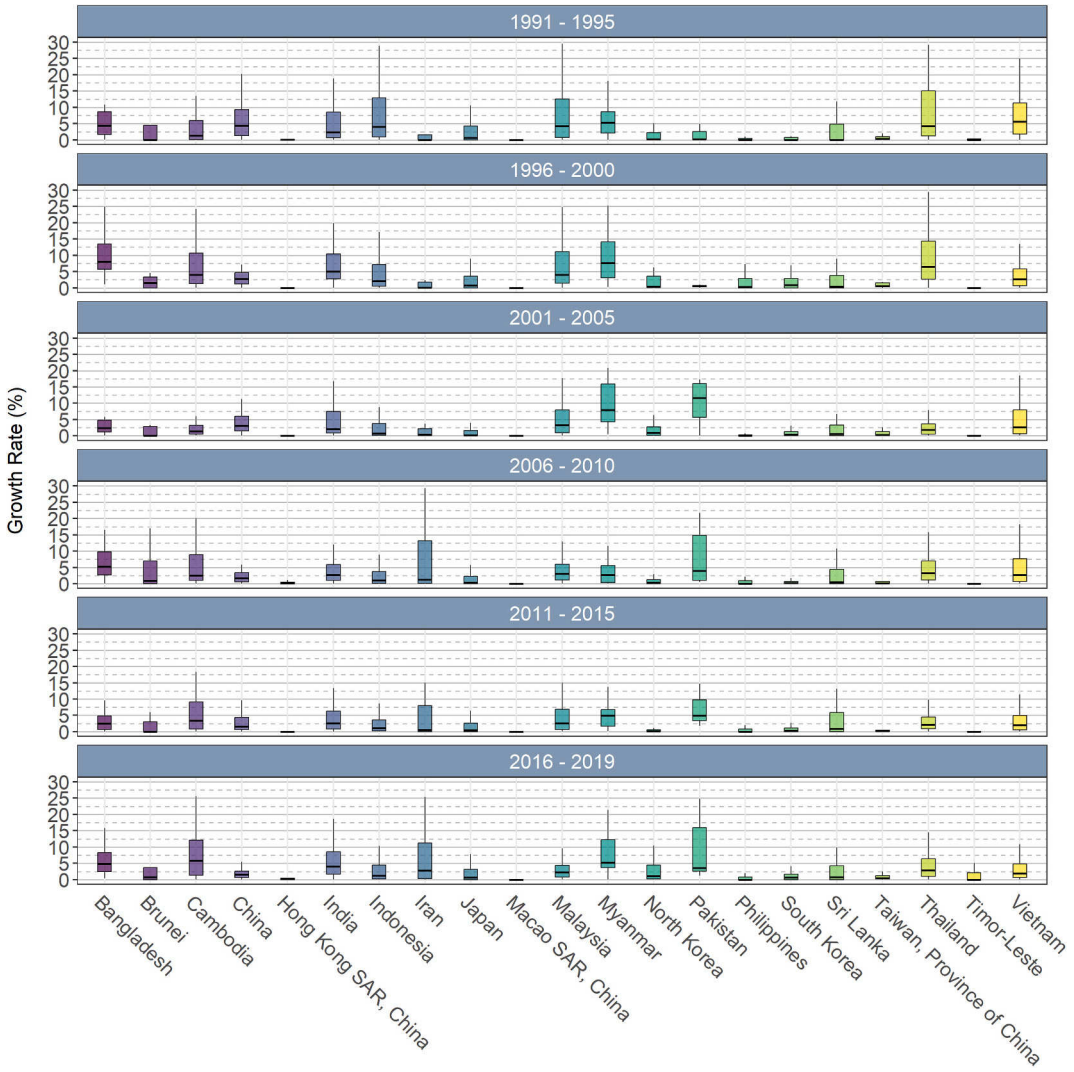

Fig. 12. Boxplots showing the 5-year average annual growth rates of the extent of active reference ponds at district level.

diminishing of regional differences between districts in terms of growth rates with respect to the spatial expansion of aquaculture ponds. Fig. 12 presents the 5-year average annual growth rates at the country level, while Fig. 14 displays the annual growth rates at the district level. The densities (ρ_{ponds}) and 10-year average annual growth rates (R_{10Y}) of the active reference pond area are presented at the district level in Fig. 14. To categorize ρ_{ponds}, we employed threshold values of 50 m^2/ha and 200 m^2/ha. Similarly, R_{10Y} was classified using threshold values of 0 % and 20 %. The densities of ponds in 1989, 2000, and 2010 were taken as the baseline situation for each observed 10-year interval. We encapsulated

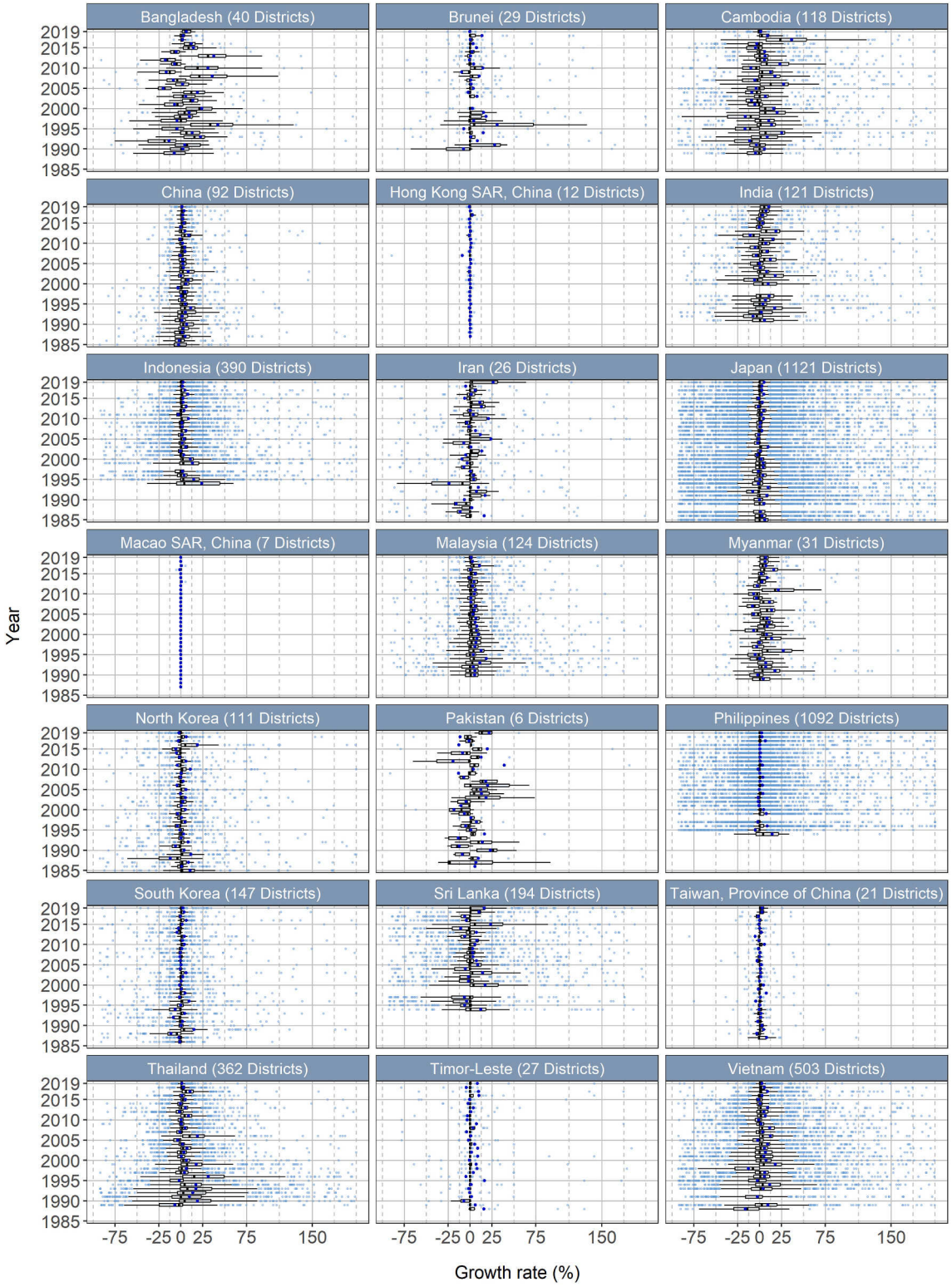

Fig. 13. Annual average annual growth rates of the extent of active coastal reference ponds at district level for each Asian country. Dark blue dots stand for the mean, light blue dots stand for outliers. (For interpretation of the references to colour in this figure legend, the reader is referred to the web version of this article.)

the spatio-temporal development of reference ponds in individual districts into nine distinct variables depending on pond area growth rate and pond area density (as illustrated in Fig. 14). It is important to note that, given the absence of a general guideline for ranking land use intensity or the growth of aquaculture production, the criteria utilized in this study are intuitive and relative. These criteria primarily were adopted for illustrating regional differences in pond aquaculture development between districts.

In South Asia (Fig. 14A), the districts exhibiting the highest pond area density and notable growth rates in all three 10-year intervals are located in the Andra Pradesh state, situated in the southern coastal region at the Indian Ocean of India. Extensive aquaculture expansion for this region has been previously documented by Prasad et al. (2019). In addition, notable growth rates during the 1990s and 2000s are observable in the hinterland of the mangrove belt of the Sundarbans in Northeast India and Bangladesh. In Maritime Southeast Asia, pond aquaculture is primarily concentrated along the north coast of northwest and northeast Java, southeast of Sumatra, and southwest and southeast of Sulawesi (Fig. 14B). In Mainland Southeast Asia, pond aquaculture production is prominently concentrated in the fertile and flat regions of the major river deltas, including the Mekong River Delta and the Red River Delta in Vietnam, the Chao Phraya Delta region around the City of Bangkok, Thailand, and the Irrawaddy River Delta in Myanmar (see Fig. 14C).

5. Discussion

To highlight the novelty of our study, we outline the key findings that distinguish our work from previous research:

- *Pan-Asian pond-level dataset*: This study presents the first dataset that tracks pond aquaculture development at the individual, object-based pond level across all of coastal Asia from the 1980s to 2019, offering insights into the evolution of aquaculture on a continental scale.
- *Cross-country comparisons*: By employing a consistent EO-based methodology, this research enables reliable comparisons of aquaculture development across 22 Asian countries, overcoming limitations over previous studies that focused on regional or national scales.
- *Advanced use of Earth Observation time series data*: Combining high-resolution Sentinel-1, Sentinel-2, and Landsat time series data, this study implements a robust and scalable method to monitor pond dynamics from a detailed 2019 reference dataset backward through decades.
- *Insights into spatio-temporal dynamics*: Detailed analysis of the pond status dataset reveal trends, growth patterns, and expansion hotspots, providing critical insights into the spatial and temporal development of aquaculture.
- *Scalable and transferable methodology*: The approach developed is scalable and transferable, making it suitable for monitoring aquaculture in regions beyond Asia.

5.1. Rapid expansion of aquaculture and its implications

Examining the period from the 1980s to 2019, it is evident that Asia has experienced substantial expansion in pond aquaculture areas across its coastal regions. The expansion patterns illustrate the dynamic evolution of pond aquaculture industry along the coasts of Asia, whose rapid growth can be attributed mainly to increasing demand for fish products (Bostock et al., 2010; Ottinger et al., 2016) and economic incentives. In 1988, the total area covered by reference ponds accounted for about 6500 km^2, while by 2019, the reference ponds covered over 19,000 km^2 of land surfaces. This represents a more than three-fold increase in the total area dedicated to pond aquaculture over the observed three decades. Among the examined countries, China utilizes by far the largest land area for pond aquaculture, followed by Indonesia, India, Vietnam and Thailand. In 1990, from the reference ponds identified as active, 42.4 % (3803 km^2) were located in China, 14.4 % in India (1290 km^2), 8.5 % in Indonesia (757 km^2), 7.5 % in Vietnam (676 km^2), 7.0 % in Thailand (630 km^2), and the remaining 20.1 % distributed across the other 17 countries. From the reference ponds identified as active in 2019, 40.6 % (7856 km^2) were located in China, 13 % in Indonesia (2661 km^2), 11.2 % in India (2176 km^2), 7.7 % in Vietnam (1492 km^2), 7.2 % in Thailand (1387 km^2), and the remaining 19.6 % distributed across Philippines, Myanmar, Bangladesh, Pakistan, Taiwan, Malaysia, South Korea, Sri Lanka, Japan, Cambodia, Iran, North Korea, Hong Kong, Brunei, Macao, and Timor-Leste.

Over the past few decades, China has emerged as a production hub in the aquaculture sector, accounting for more than 40 % of the total share of active pond area. Indonesia and India follow with 13 % and 11.2 % shares of the total active aquaculture ponds detected in our analyses. It is noteworthy that India's share of active ponds was higher in 1990 (14.4 %) than Indonesia's (8.5 %), but Indonesia has since surpassed India in active reference pond area. All three top producer countries demonstrate high growth rates of aquaculture pond area in their coastal regions, with an overall growth rate from 1990 to 2019 of 69.8 % for China, 40.7 % for India, and 71.5 % for Indonesia. In contrast, Malaysia demonstrated slight and steady growth in pond aquaculture throughout the entire observation period. According to Duan et al. (2021), China's aquaculture industry has undergone distinct phases, including rapid expansion before 2011, a period of stability spanning 2011 to 2017, and a decline in post-2017. According to analysis by Ying and Ying (2023), China's contribution to world's aquaculture production is forecasted to decrease marginally by the year 2030 which is attributed to the sustained implementation of the 13th Five-Year Plan's initiatives aimed at reducing fishing and aquaculture activities.

The rapid expansion of pond aquaculture in Asia since the 1980s is attributed to three main causes: (i) increasing demand for fish products (Belton and Thilsted, 2014; Béné et al., 2016; Béné et al., 2015; Boyd et al., 2022; Naylor, 2016), (*ii*) economic incentives (Anderson et al., 2019; Kumar et al., 2018; Naylor et al., 2023), and (*iii*) governmental policies promoting the industry. This growth has led to large-scale land-use changes, resulting in the conversion of natural habitats, such as mangroves, to aquaculture ponds (Heimann and Delzeit, 2024; Ottinger et al., 2016). This conversion has severe consequences, including loss of biodiversity and coastal protection, as well as increased greenhouse gas emissions (Ahmed and Glaser, 2016; Ballut-Dajud et al., 2022). The expansion has also raised concerns about environmental sustainability, including water pollution (Ahmed and Thompson, 2019), habitat degradation (Sampantamit et al., 2020), and disease spread (Maulu et al., 2021). Furthermore, it has led to increased competition for land and freshwater resources uses (Henriksson et al., 2021; Pueppke et al., 2020), potentially exacerbating conflicts over natural resources. The implications of these changes are far-reaching, and understanding the causes and consequences of aquaculture expansion is crucial for informing policy and promoting sustainable development in the sector. Studies highlight the need to expand aquaculture to meet growing demand, while cautioning about the social, economic, and environmental costs of this growth (Boyd et al., 2022; Garlock et al., 2024). To mitigate the negative effects of aquaculture, new policies and regulations may be required. A balanced approach that considers the economic, social, and environmental aspects of aquaculture development is necessary to ensure the long-term sustainability of the industry.

5.2. Comparison of pond aquaculture area and official aquaculture production statistics

Our study provides a novel methodological approach, offering the first pan-Asian, pond-level analysis of aquaculture development using Earth Observation data. Additionally, it enables consistent comparisons across countries, enabling comprehensive regional assessments and

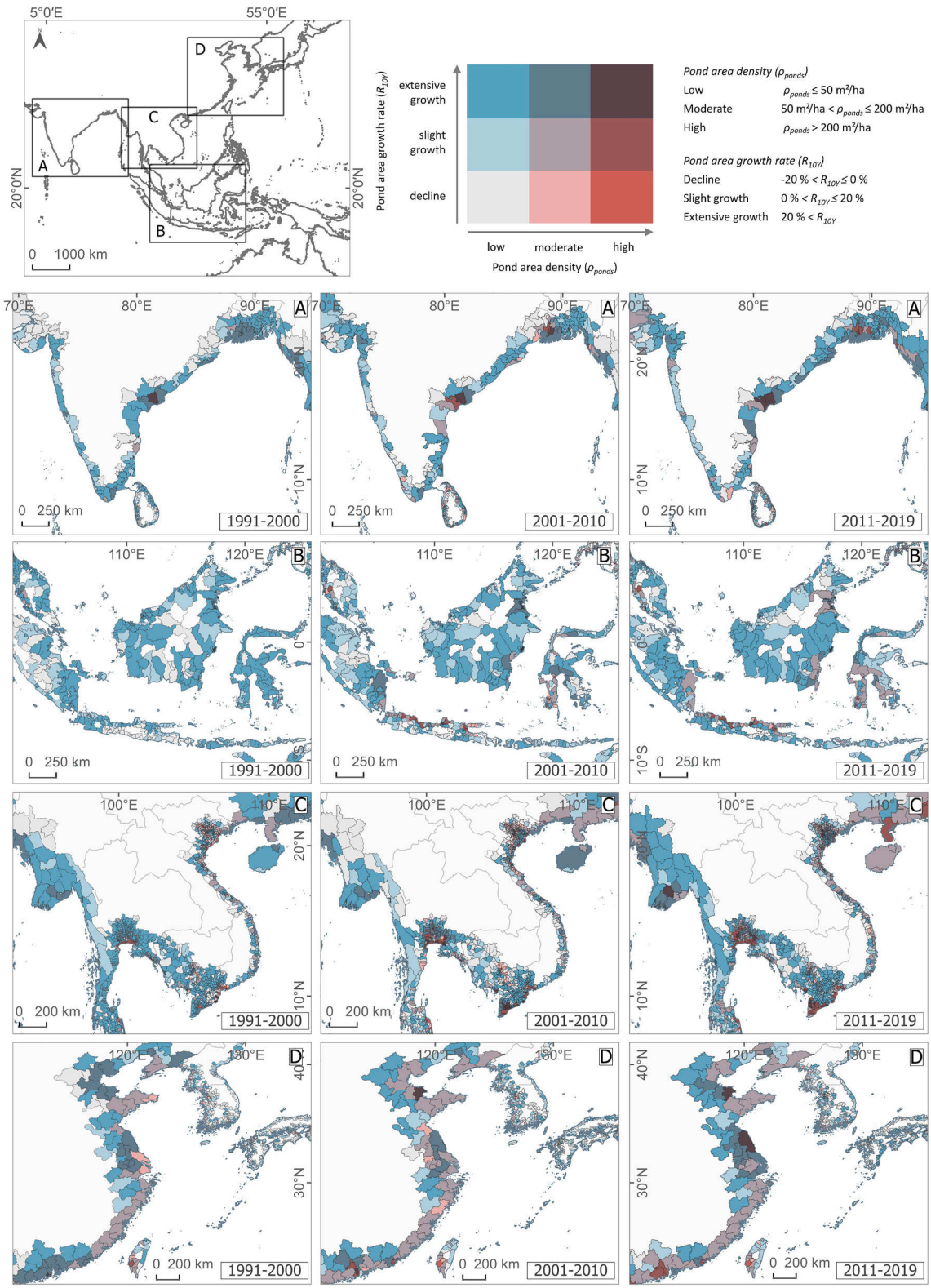

Fig. 14. Bivariate map of density and 10-year average annual growth of active reference ponds in detailed submaps for (A) South Asia covering India, Sri Lanka, and Bangladesh, (B) Southeast Asia Maritime covering Indonesia and Malaysia (C) Southeast Asia Mainland covering Myanmar, Thailand, Cambodia and Vietnam and (D) East Asia covering China, Taiwan, South and North Korea and Japan. For each submap the growth rates are shown for the 1990s (left), the 2000s (center) and the 2010s (right).

policy implications. To further validate our results, we compared our results on pond aquaculture area with official reported statistical data provided by the FAO (FAO, 2023) on aquaculture production, and created a graph (see Fig. 15) illustrating the annual aquaculture production in tonnes alongside the area of active reference ponds for each country from the late 1980s to 2019. This comparison is intended as an

illustrative visualization rather than verification, as historical pond area data is likely underestimated due to study design limitations. Since FAO's aquaculture databases do not provide system-specific production, it is not possible to isolate pond aquaculture production from other forms of aquaculture at the national level. These production statistics cover all land-based aquaculture systems, not just ponds (Ottinger et al., 2016), but ponds dominate coastal aquaculture in Asia.

We observed that the expansion of pond areas generally relates with increasing production in countries like China, India, Vietnam, and Myanmar. However, the relationship between the expansion of reference ponds and production is not always aligned, suggesting other factors influence production, such as farming practices, technology adoption, market dynamics, delayed reporting, or external events like environmental conditions, animal diseases, pandemic triggered economic crisis, or policy interventions. For example, Thailand's notable decline in production since 2010, specifically shrimp farming, is not reflected in the time series of reference pond areas, likely due to infectious disease outbreaks (Sampantamit et al. (2020)). Similarly, the Philippines saw a 10 % decline in shrimp production over the last decade, due to bacterial diseases and viral infections (e.g. white spot syndrome) (Mialhe et al., 2016). Conversely, Indonesia's production growth since 2005 onwards does not clearly reflect the growth rates of active ponds primarily between 1990 and 2005, suggesting that the later increase in production may be attributed to a delayed intensification of aquaculture practices. Overall, aquaculture yields are influenced by various factors, including climate and meteorological conditions, water quality, and disease outbreaks. For instance, Cambodia's rapid production growth from 26,000 t in 2005 to more than 305,000 t in 2019 does not correspond with reference pond area growth. These discrepancies highlight the complexity of aquaculture dynamics beyond just pond area expansion.

5.3. Data availaibility, data quality and accuracy

The accuracy and reliability of the data sources and methodologies used to generate the time series for both reference pond areas and aquaculture yields are crucial. Discrepancies between the trends observed in the reference pond data and the actual aquaculture production may require a more detailed analysis of influencing factors and methods. Our study found no evidence that larger pond areas correlate with higher accuracies in the water status determination. Instead, accuracy depends on factors such as quality of the reference data, satellite data resolution and coverage, and the data processing methods used. The quality of the pond reference data is critical for the accurate water status determination. Higher spatial and temporal reference data can improve the accuracy, provide more accurate water masks, and enhance the overall performance of the water status determination. However, continuous and free accessible space-borne SAR missions with higher resolution do not yet exist. Such data would enhance capabilities for object detection of small surface features like aquaculture ponds. Satellite data coverage is also important - areas with poor data coverage may result in less accurate water status determination. In our study, most land areas had more than 250 images for the investigated study period, which were sufficient for generating annual water masks, although areas with poor data coverage showed lower accuracy.

Fig. 16 illustrates that the accuracy of water status determination varies with pond size, showing better performance for larger ponds. The analysis of false negative (FN) and true positive (TP) classified ponds highlights this difference (Fig. 16), as FN ponds tend to be smaller, with an average size of 340 square meter, while TP ponds are larger, averaging 1040 square meter. Given that a single Landsat pixel (30 m x 30 m) covers 900 square meters, which is larger than most reference ponds, this suggests that ponds larger than one Landsat pixel are more likely to be classified accurately. Smaller ponds, however, show more variable classification results. The box plots further illustrate the size distribution of ponds across different countries, emphasizing this relationship between pond size and classification accuracy. A summary of pond metrics across the countries in the study region is provided in Table 4, detailing the number of reference ponds, share of active ponds, average pond size, mean pond compactness, and mean pond convex hull area. These metrics provide critical context for understanding the variability in pond characteristics and their influence on classification accuracy.

Landscape-specific conditions can also pose challenges in accurately capturing pond data using EO methods. For example, in Bangladesh, discrepancies between official production statistics and active pond area are evident, particularly given its ranking as the 5th largest global producer according to FAO statistics, compared to 10th in our analysis. The prevalence of small-scale fish farms (Rahman et al., 2022) can influence the detection with EO data of 10 m spatial resolution. Additionally, the high proportion of mangroves complicates the radar-based segmentation of individual ponds due to increased scattering and double bounce effects (Ottinger and Kuenzer, 2020). Furthermore, significant data gaps exist in Landsat-4 and Landsat-5 imagery during the late 1980s and early 1990s limit the quality of water masks from that period, compared to the more robust data volume available with the Landsat-7, Landsat-8 and Landsat-9 satellites.

5.4. Limitations of the study approach

The monitoring approach developed in this study, focusing on aquaculture development based on reference ponds, has certain limitations. One key limitation is that pond objects were not separately detected and extracted for all observed years. This decision stems from the methodology used to prepare the reference dataset (Ottinger et al. (2022)), which relies on high spatial and temporal satellite time series to extract pond shapes based on backscatter signals, enhanced with optical features to separate aquaculture from non-aquaculture objects. Sentinel-1 SAR data, providing global 10 m resolution and free accessibility, was used for pond mapping due to its ability to provide dense time series for the entire coastal zone of Asia. This enabled the detection of small pond objects by identifying smooth surfaces and separating stable, water-covered aquaculture ponds from other water bodies. However, the lack of continuous, high-resolution, weather-independent satellite data before 2016 (corresponds to the start of Sentinel-1 twin operation mode) limits the ability to detect pond boundary information for earlier years and accurately track pond boundary changes over time at the single-pond level. While commercial very high resolution satellite data could be applied to smaller study sites, using such data for the vast coastal zone of Asia with an area of over 6 million square kilometers analyzed in this study is impractical due to limited swath width and mapping capabilities.

The performance of this method also dependents on the quality of the reference dataset. Ponds not included in the reference dataset could not be observed in historical Landsat time series. Additionally, identifying pond status in earlier years (prior to the 2019) may lead to false positives, as reference ponds might be misclassified as active ponds if covered by non-aquaculture water bodies. Furthermore, the method cannot account for ponds abandoned before the reference year (2019), which restricts the ability to observe historical ponds. As a result, the spatiotemporal patterns presented in this study should be interpreted with caution due to potential biases.

5.5. The role of remote sensing in supporting sustainable planning and management

This paper advances the role of remote sensing in aquaculture planning and management by demonstrating its application at a continental scale to address challenges in sustainable aquaculture. While planning and management often occur at localized levels, our work provides a macro-level perspective essential for strategic planning and decision-making for regional and national policymakers, international organizations, environmental agencies, among others. By providing a

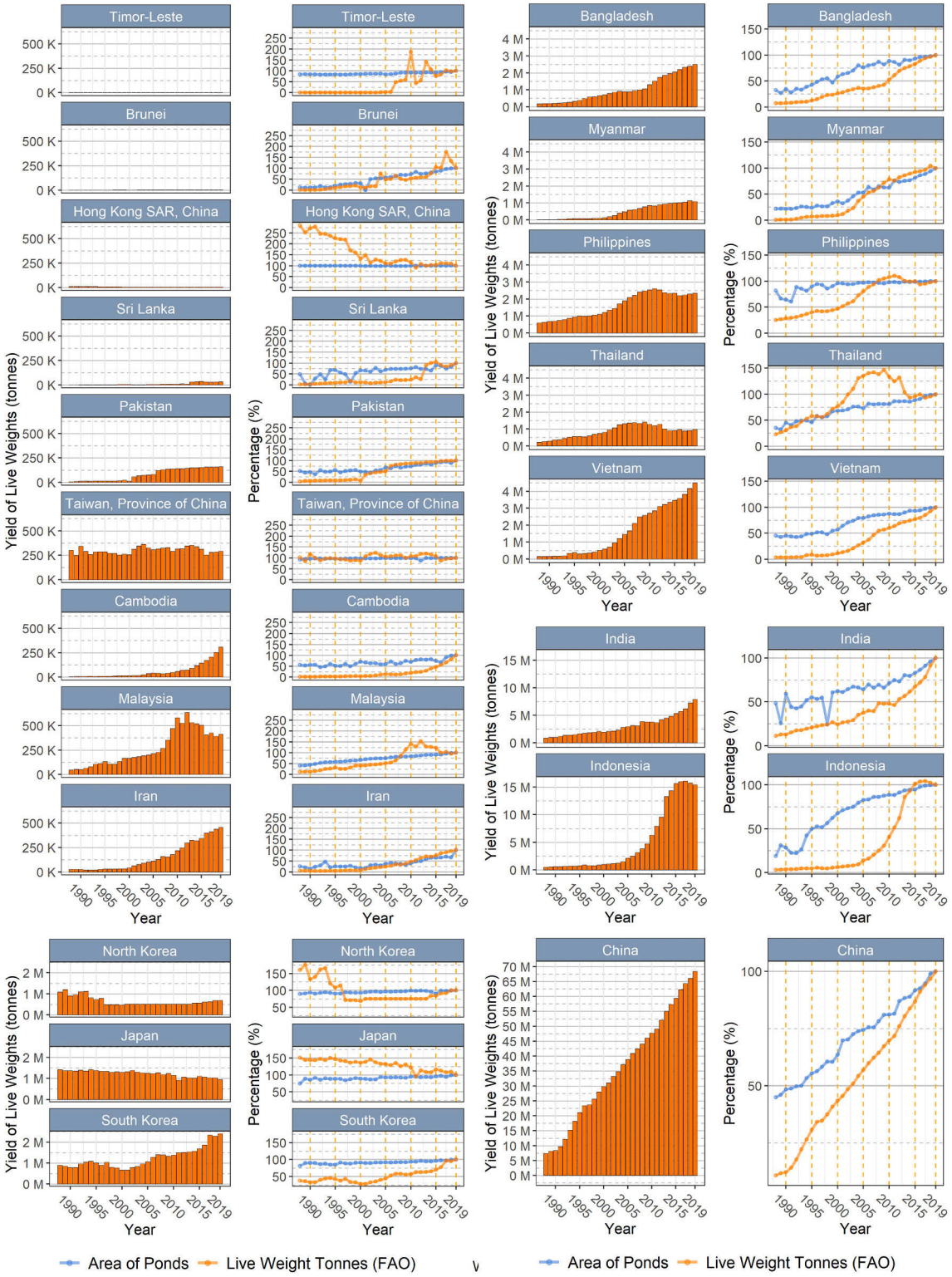

Fig. 15. First and third column: Yearly extent of active reference ponds by country; Second and fourth column: Blue line - Percentage difference between each year's active pond area and the area of all reference ponds in 2019 (100 %) by country; Orange line - Percentage difference between each year's production and the production in 2019 (100 %) by country. FAO-reported aquaculture production: aquaculture products excluding aquatic photosynthetic organism. (For interpretation of the references to colour in this figure legend, the reader is referred to the web version of this article.)

broad overview of aquaculture dynamics, our study significantly expands the application of remote sensing in sustainable aquaculture by offering unique contributions. For example, the large-scale pond status dataset enables the identification of land-use conflicts and the assessment of aquaculture-related impacts on conservation areas, such as mangrove loss. It also facilitates monitoring of climate change impacts, including water temperature changes, trends and their effects on production and disease outbreaks, thereby contributing to more sustainable aquaculture practices. The reference pond objects with their spatio-temporal water status information derived from this study have the

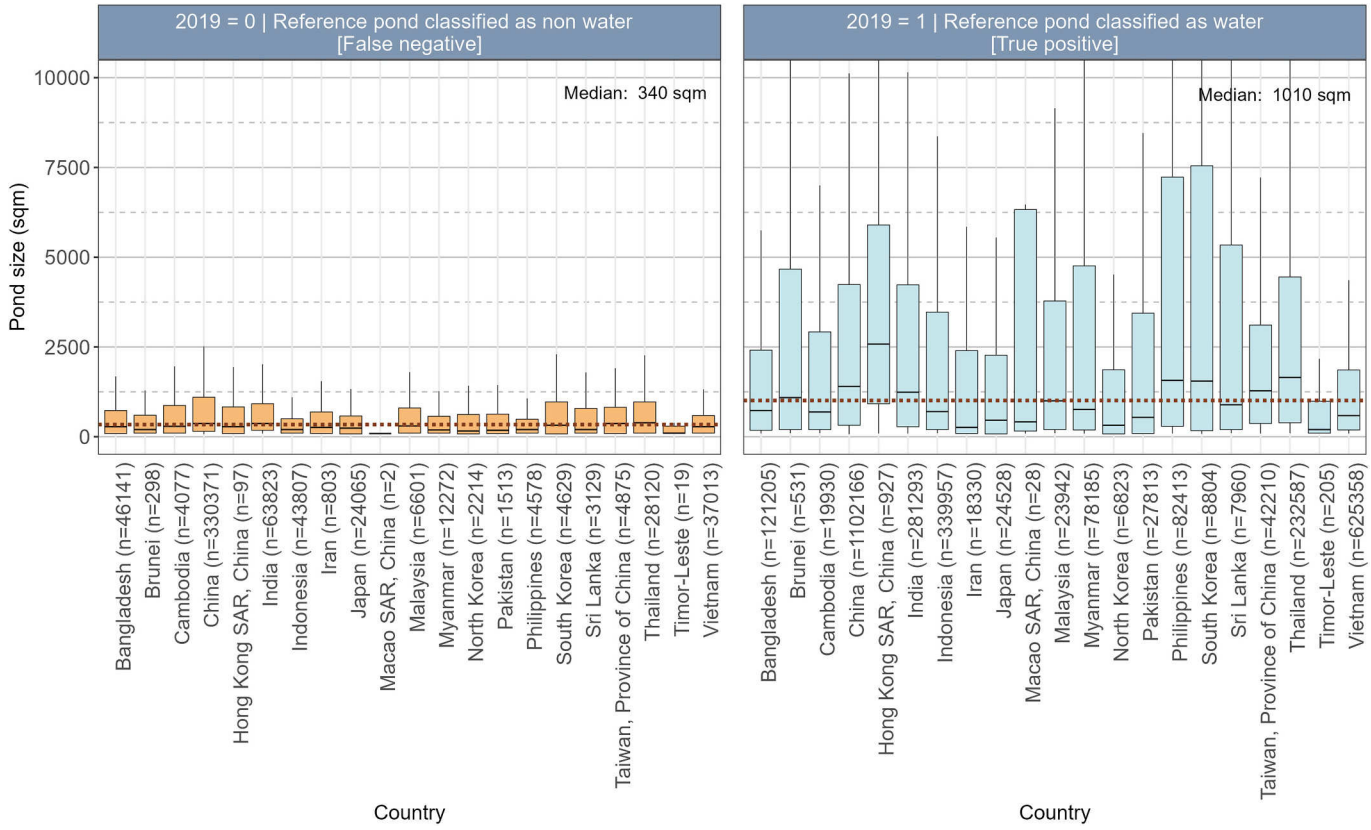

Fig. 16. Analysis of 2019 reference pond status accuracy. Comparison of accurately identified reference ponds (right) vs. unidentified reference ponds which were not identified for the year 2019 (left) based on the annual 2019 Landsat water masks. Box plots show the distribution of pond sizes by country.

Table 4
Summary of pond metrics across countries of the study region. Pond metrics include: number of reference ponds, share of active ponds, average pond size, mean pond compactness, mean pond convex hull area.

Country	Number of reference ponds in 2019	Active reference ponds in 2019[1]	Share of active ponds in 2019 (%)[2]	Average pond size (sqm)[3]	Mean compactness[4]	Mean convex hull area to pond area ratio[5]
Bangladesh	167,346	121,205	72.4	868	0.58	0.75
Brunei Darussalam	829	531	64.1	6169	0.56	0.86
Cambodia	24,007	19,930	83.0	1175	0.56	0.83
China[1]	1,432,575	1,102,166	76.9	1626	0.53	0.66
Dem. People's Rep. Korea	9037	6823	75.5	784	0.58	0.54
Hong Kong SAR, China	1024	927	90.5	2617	0.51	0.73
India	345,116	281,293	81.5	1666	0.54	0.78
Indonesia	383,805	339,957	88.6	1474	0.55	0.86
Iran	19,209	18,330	95.4	1252	0.58	0.66
Japan	48,594	29,528	60.7	562	0.59	0.59
Macao SAR, China	30	28	93.3	16,677	0.54	0.77
Malaysia	30,543	23,942	78.4	1393	0.55	0.86
Myanmar	90,476	78,185	86.4	1975	0.55	0.79
Pakistan	29,326	27,813	94.8	1683	0.55	0.72
Philippines	86,991	82,413	94.7	3199	0.51	0.81
Republic of Korea	13,434	8804	65.5	1937	0.54	0.58
Sri Lanka	11,089	7960	71.8	1787	0.55	0.88
Taiwan, Province of China	47,085	42,210	89.6	1419	0.54	0.73
Thailand	260,713	232,587	89.2	2013	0.52	0.82
Timor-Leste	224	205	91.5	427	0.61	0.87
Vietnam	662,390	625,358	94.4	867	0.57	0.83
Asia total (22 countries)	3,663,843	3,050,195	82.7	1426	0.55	0.76

[1] Reference Ponds with active water status in 2019 (determined using Landsat water masks).
[2] Share of classified active ponds compared to the total number of reference ponds in 2019 (in percent).
[3] Average pond size in square meters (sqm) calculated by the 90th percentile mean.
[4] Mean pond compactness per country for reference ponds in 2019. For details see: Ottinger et al. (2022).
[5] Mean convex hull area to pond area ratio per country for reference ponds in 2019. For details see: Ottinger et al. (2022).

potential to be combined with other environmental datasets – such as information on land use, water quality and temperature, pollutants, and conservation areas – to create a comprehensive and holistic view of aquaculture production. Key applications include:

- Mapping land-use changes to and from aquaculture, including abandoned pond detection and classification.
- Integrating multi- and hyperspectral data, alongside climate simulations, to monitor pond-level water quality and detect pollution.
- Identifying pollution hotspots from intensive aquaculture regions to mitigate environmental impacts.
- Quantifying mangrove loss due to pond expansion as well as considering climate change impacts on mangroves and aquaculture.

While EO data offers large-scale insights, detailed fieldwork remains essential for thorough site-specific analysis, particularly for accurately identifying pollution hotspots and conducting precise water and sediment assessments (Braun et al., 2019). Enhancements in continuous high-resolution satellite data availability, coupled with advancements in processing and object and feature detection capabilities, will enhance the analysis of environmental impacts. This will support the monitoring of environmental compliance of the aquaculture food supply chains and significantly improve the sustainability and transparency of aquaculture practices.

6. Conclusion

This paper presents an EO-based approach for high-resolution monitoring of land-based aquaculture in coastal Asia, focusing on individual ponds. It offers a comprehensive spatio-temporal analysis pond aquaculture development across the region. By processing multi-decadal Landsat archive data, a framework was developed for annual pond status assessment from 2019 (pond reference dataset) back to the 1980s. The reference dataset for 2019 was created using time series data from the European EO missions Sentinel-1 and Sentinel-2. The object-based, pond-level analysis of annual aquaculture status, derived from satellite time series, provides novel, detailed insights into the spatio-temporal development of pond aquaculture across the continent, revealing trends over time.

The study found significant expansion in pond aquaculture over the past three decades. From 1980 to 2019, the active pond area more than doubled, reaching 19,000 km^2 in 2019. This growth can be attributed to increasing demand for fish products and economic incentives. China, the largest pond aquaculture producer, maintained its dominant position, accounting for over 40 % of the total active pond area in 2019, followed by Indonesia, India, Vietnam, and Thailand. However, the expansion of pond aquaculture has been accompanied by challenges, including disease outbreaks and environmental pollution, leading to production declines in recent years. Additionally, the rapid growth has resulted in disturbances to natural coastal ecosystems and protective coastal vegetation barriers, including mangroves and wetlands. China's pond aquaculture industry has experienced significant growth, while Indonesia surpassed India in active pond area over the last three decades. The analysis of mean annual growth rates for 5- and 10-year intervals in this study highlights regional differences in development patterns across the studied countries.

Further research is needed to assess the long-term sustainability of the pond aquaculture industry in Asia. The performance of the method applied depends on the quality of the reference dataset, which can result in false positives if reference ponds are later replaced by non-aquaculture water-bodies. Abandoned ponds that existed in earlier years but were abandoned prior to the reference pond sampling cannot be observed. Furthermore, long-term time series derived from Earth Observation with higher temporal (<14d) and higher spatial (<30 m) resolution than Landsat could enhance our understanding of the aquaculture-ecosystem nexus.

This study provides a pond-level analysis for the entire pan-Asian coast, a level of detail that has not been available before. By conducting geostatistical analysis of pond development and comparing these findings with FAO production statistics, our study offers a comprehensive, large-scale assessment of pond dynamics across 22 countries. This kind of analysis has not been conducted previously at this scale. The ability to process large volumes of EO data allows for reliable, consistent analysis, with scalability for application to other regions or scales. In conclusion, continuous EO-based monitoring of aquaculture areas enhances our understanding of pond aquaculture dynamics, supporting informed decision-making regarding sustainability and resource management. The comprehensive, continental-wide pond dataset developed in this study provides an essential foundation for future research and decision-making, helping to ensure economic and environmental sustainability of pond aquaculture.

Funding sources

Preparatory data analysis for the Southeast Asia region were partly funded by the German Ministry of Education and Research (BMBF) through the FloodAdapt project (grant No. 01LE1905A1).

Authorship contribution statement

Marco Ottinger: Conceptualization, Methodology, Software, Formal Analysis, Visualization, Writing – original draft; Kemeng Liu: Methodology, Software, Visualization; Writing – review and editing; Tobias Ullmann: Methodology; Validation; Writing – review & editing; Juliane Huth: Conceptualization; Methodology; Writing – review & editing; Claudia Kuenzer: Writing – review & editing; Felix Bachofer: Conceptualization; Methodology; Writing – review & editing;

Software and data processing

For processing the satellite data, annual water masks, reference pond vector dataset, and administrative boundary layers, we used Python (version 3.8) for code scripting including following packages: earthengine-api (0.1.252), rasterstats (0.17.0), rioxarray (0.12.2), pandas (1.2.2), geopandas (0.8.2), geofeather (0.3.0), joblib (1.2.0). Multi—core processing. For the line graphs, scatter plots and pie charts, we used R and Python. To perform parallel processing for calculating the water status across all coastal parcels for all years, we used the multiprocessing package in Python on a local CPU-server machine.

Please contact the German Aerospace Center, DLR (marco.ottinger@dlr.de) upon request about the pond aquaculture dynamics dataset.

CRediT authorship contribution statement

Marco Ottinger: Methodology, Visualization, Writing – original draft, Software, Conceptualization, Formal analysis. **Kemeng Liu:** Methodology, Software, Writing – review & editing, Visualization. **Tobias Ullmann:** Writing – review & editing, Methodology, Validation. **Juliane Huth:** Conceptualization, Methodology, Writing – review & editing. **Claudia Kuenzer:** Writing – review & editing. **Felix Bachofer:** Conceptualization, Methodology, Writing – review & editing.

Declaration of competing interest

The authors declare the following financial interests/personal relationships which may be considered as potential competing interests:

Kemeng Liu reports financial support was provided by Federal Ministry of Education and Research. If there are other authors, they declare that they have no known competing financial interests or personal relationships that could have appeared to influence the work reported in this paper.

Acknowledgements

Special thanks go to the United States Geological Survey (USGS) and the National Aeronautics and Space Administration (NASA) for the Landsat program as well as the Copernicus Satellite Program for providing free access to the global Landsat archive and Sentinel-1 and Sentinel-2 data; the NASA JPL for providing the free SRTM version 3 dataset; the Open Street Map project for providing free data on waterbodies and shorelines; and GADM for providing data on administrative areas. Furthermore, we would like to thank the Google Earth Engine platform for generating and providing the satellite time series, and we would also like to thank G. Donchyts for the thresholding function available in GEE. Finally, we would like to thank the FAO for providing updated global aquaculture statistics.

Data availability

Data will be made available on request.

References

Ahmed, N., Glaser, M., 2016. Coastal aquaculture, mangrove deforestation and blue carbon emissions: is REDD+ a solution? Mar. Policy 66, 58–66. https://doi.org/10.1016/j.marpol.2016.01.011.

Ahmed, N., Thompson, S., 2019. The blue dimensions of aquaculture: a global synthesis. Sci. Total Environ. 652, 851–861. https://doi.org/10.1016/j.scitotenv.2018.10.163.

Akber, Md.A., Aziz, A.A., Lovelock, C., 2020. Major drivers of coastal aquaculture expansion in Southeast Asia. Ocean Coast. Manag. 198, 105364. https://doi.org/10.1016/j.ocecoaman.2020.105364.

Anderson, J.L., Asche, F., Garlock, T., 2019. Economics of aquaculture policy and regulation. Ann. Rev. Resour. Econ. 11, 101–123. https://doi.org/10.1146/annurev-resource-100518-093750.

Aslan, A., Rahman, A.F., Robeson, S.M., Ilman, M., 2021. Land-use dynamics associated with mangrove deforestation for aquaculture and the subsequent abandonment of ponds. Sci. Total Environ. 791, 148320. https://doi.org/10.1016/j.scitotenv.2021.148320.

Ballut-Dajud, G.A., Sandoval Herazo, L.C., Fernández-Lambert, G., Marín-Muñiz, J.L., López Méndez, M.C., Betanzo-Torres, E.A., 2022. Factors affecting wetland loss: a review. Land 11, 434. https://doi.org/10.3390/land11030434.

Belton, B., Little, D., 2008. The Development of Aquaculture in Central Thailand: Domestic Demand versus Export-Led Production. J. Agrar. Change. 8 (1), 123–143. https://doi.org/10.1111/j.1471-0366.2007.00165.x.

Belton, B., Thilsted, S.H., 2014. Fisheries in transition : food and nutrition security implications for the global south. Glob. Food Sec. 3, 59–66. https://doi.org/10.1016/j.gfs.2013.10.001.

Belton, B., Padiyar, A., Ravibabu, G., Gopal Rao, K., 2017. Boom and bust in Andhra Pradesh: development and transformation in India's domestic aquaculture value chain. Aquaculture 470, 196–206. https://doi.org/10.1016/j.aquaculture.2016.12.019.

Béné, C., Barange, M., Subasinghe, R., Pinstrup-Andersen, P., Merino, G., Hemre, G.-I., Williams, M., 2015. Feeding 9 billion by 2050 – putting fish back on the menu. Food Secur. 261–274. https://doi.org/10.1007/s12571-015-0427-z.

Béné, C., Arthur, R., Norbury, H., Allison, E.H., Beveridge, M., Bush, S., Campling, L., Leschen, W., Little, D., Squires, D., Thilsted, S.H., Troell, M., Williams, M., 2016. Contribution of fisheries and aquaculture to food security and poverty reduction: assessing the current evidence. World Dev. 79, 177–196. https://doi.org/10.1016/j.worlddev.2015.11.007.

Boyd, C.E., McNevin, A.A., Davis, R.P., 2022. The contribution of fisheries and aquaculture to the global protein supply. Food Sec. 14, 805–827. https://doi.org/10.1007/s12571-021-01246-9.

Braun, G., Braun, M., Kruse, J., Amelung, W., Renaud, F.G., Khoi, C.M., Duong, M.V., Sebesvari, Z., 2019. Pesticides and antibiotics in permanent rice, alternating rice-shrimp and permanent shrimp systems of the coastal Mekong Delta, Vietnam. Environ. Int. 127, 442–451. https://doi.org/10.1016/j.envint.2019.03.038.

Canny, J., 1986. A computational approach to edge detection. In: IEEE Transactions on Pattern Analysis and Machine Intelligence PAMI-8. https://doi.org/10.1109/TPAMI.1986.4767851.

Dauda, A.B., Ajadi, A., Tola-Fabunmi, A.S., Akinwole, A.O., 2019. Waste production in aquaculture: sources, components and managements in different culture systems. Aquacul. Fish. 4, 81–88. https://doi.org/10.1016/j.aaf.2018.10.002.

Duan, Y., Tian, B., Li, X., Liu, D., Sengupta, D., Wang, Y., Peng, Y., 2021. Tracking changes in aquaculture ponds on the China coast using 30 years of Landsat images. Int. J. Appl. Earth Obs. Geoinf. 102, 102383. https://doi.org/10.1016/j.jag.2021.102383.

European Commission, Joint Research Centre, 2015. GHS-POP R2015A - GHS population grid, derived from GPW4.

FAO, 2021. Fishery and aquaculture statistics. Global aquaculture production 1950-2019 (FishstatJ). In: FAO Fisheries Division [Online]. Rome (Updated June 2021).

FAO, 2023. Fishery and aquaculture statistics. global aquaculture production 1950–2021 (FishStatJ). In: FAO Fisheries and Aquaculture Division [online]. Rome. Updated 2023.

Feyisa, G.L., Meilby, H., Fensholt, R., Proud, S.R., 2014. Automated water extraction index: a new technique for surface water mapping using Landsat imagery. Remote Sens. Environ. 140, 23–35. https://doi.org/10.1016/j.rse.2013.08.029.

Fisher, A., Flood, N., Danaher, T., 2016. Comparing Landsat water index methods for automated water classification in eastern Australia. Remote Sens. Environ. 175, 167–182. https://doi.org/10.1016/j.rse.2015.12.055.

Fu, Y., Deng, J., Ye, Z., Gan, M., Wang, K., Wu, J., Yang, W., Xiao, G., 2019. Coastal aquaculture mapping from very high spatial resolution imagery by combining object-based neighbor features. Sustainability 11, 637. https://doi.org/10.3390/su11030637.

Fu, T., Zhang, L., Yuan, X., Chen, B., Yan, M., 2021. Spatio-temporal patterns and sustainable development of coastal aquaculture in Hainan Island, China: 30 years of evidence from remote sensing. Ocean Coast. Manag. 214, 105897. https://doi.org/10.1016/j.ocecoaman.2021.105897.

GADM, 2012. Global Administrative Areas (2012). GADM database of Global Administrative Areas, version 2.0. [online].

Garlock, T.M., Asche, F., Anderson, J.L., Eggert, H., Anderson, T.M., Che, B., Chávez, C. A., Chu, J., Chukwuone, N., Dey, M.M., Fitzsimmons, K., Flores, J., Guillen, J., Kumar, G., Liu, L., Llorente, I., Nguyen, L., Nielsen, R., Pincinato, R.B.M., Sudhakaran, P.O., Tibesigwa, B., Tveteras, R., 2024. Environmental, economic, and social sustainability in aquaculture: the aquaculture performance indicators. Nat. Commun. 15, 5274. https://doi.org/10.1038/s41467-024-49556-8.

Gorelick, N., Hancher, M., Dixon, M., Ilyushchenko, S., Thau, D., Moore, R., 2017. Google earth engine: planetary-scale geospatial analysis for everyone. Remote Sensing of Environment, Big Remotely Sensed Data: tools, applications and experiences 202, 18–27. https://doi.org/10.1016/j.rse.2017.06.031.

Hay, G.J., Blaschke, T., Marceau, D.J., Bouchard, A., 2003. A comparison of three image-object methods for the multiscale analysis of landscape structure. ISPRS J. Photogramm. Remote Sens. 57, 327–345. https://doi.org/10.1016/S0924-2716(02)00162-4.

Heimann, T., Delzeit, R., 2024. Land for fish: quantifying the connection between the aquaculture sector and agricultural markets. Ecol. Econ. 217, 108090. https://doi.org/10.1016/j.ecolecon.2023.108090.

Henriksson, P.J.G., Troell, M., Banks, L.K., Belton, B., Beveridge, M.C.M., Klinger, D.H., Pelletier, N., Phillips, M.J., Tran, N., 2021. Interventions for improving the productivity and environmental performance of global aquaculture for future food security. One Earth 4, 1220–1232. https://doi.org/10.1016/j.oneear.2021.08.009.

Herbeck, L.S., Krumme, U., Andersen, T.J., Jennerjahn, T.C., 2020. Decadal trends in mangrove and pond aquaculture cover on Hainan (China) since 1966: mangrove loss, fragmentation and associated biogeochemical changes. Estuar. Coast. Shelf Sci. 233, 106531. https://doi.org/10.1016/j.ecss.2019.106531.

Jiang, Y., Li, J., Zhang, Z., Li, Y., 2024. Dynamics of coastal land-based aquaculture pond in China and Southeast Asia from 1990 to 2020. Int. J. Appl. Earth Obs. Geoinf. 127, 103654. https://doi.org/10.1016/j.jag.2024.103654.

Kumar, G., Engle, C., Tucker, C., 2018. Factors driving aquaculture technology adoption. J. World Aquacult. Soc. 49, 447–476. https://doi.org/10.1111/jwas.12514.

Li, C.H., Lee, C.K., 1993. Minimum cross entropy thresholding. Pattern Recogn. 26, 617–625. https://doi.org/10.1016/0031-3203(93)90115-D.

Liu, J., Li, D., Li, W., Sui, H., 2006. Automatic thresholding for edge detection in Sar imagery. In: ISPRS Commision VII Mid-term … 2–5.

Loc, V.T.T., Bush, S.R., Sinh, L.X., Khiem, N.T., 2010. High and low value fish chains in the Mekong Delta: challenges for livelihoods and governance. Environ. Dev. Sustain. 12, 889–908. https://doi.org/10.1007/s10668-010-9230-3.

Luo, J., Sun, Z., Lu, L., Xiong, Z., Cui, L., Mao, Z., 2022. Rapid expansion of coastal aquaculture ponds in Southeast Asia: patterns, drivers and impacts. J. Environ. Manag. 315, 115100. https://doi.org/10.1016/j.jenvman.2022.115100.

Maulu, S., Hasimuna, O.J., Haambiya, L.H., Monde, C., Musuka, C.G., Makorwa, T.H., Munganga, B.P., Phiri, K.J., Nsekanabo, J.D., 2021. Climate change effects on aquaculture production: sustainability implications, mitigation, and adaptations. Front. Sustain. Food Syst. 5, 70. https://doi.org/10.3389/fsufs.2021.609097.

McFeeters, S.K., 1996. The use of the normalized difference water index (NDWI) in the delineation of open water features. Int. J. Remote Sens. 17, 1425–1432. https://doi.org/10.1080/01431169608948714.

McSherry, M., Davis, R.P., Andradi-Brown, D.A., Ahmadia, G.N., Van Kempen, M., Wingard Brian, S., 2023. Integrated mangrove aquaculture: the sustainable choice for mangroves and aquaculture? Front. For. Glob. Change 6, 1094306. https://doi.org/10.3389/ffgc.2023.1094306.

Mialhe, F., Gunnell, Y., Mering, C., Gaillard, J.-C., Coloma, J.G., Dabbadie, L., 2016. The development of aquaculture on the northern coast of Manila Bay (Philippines): an analysis of long-term land-use changes and their causes. J. Land Use Sci. 11, 236–256. https://doi.org/10.1080/1747423X.2015.1057245.

Naylor, R.L., 2016. Oil crops, aquaculture, and the rising role of demand: a fresh perspective on food security. Glob. Food Sec. 11, 17–25. https://doi.org/10.1016/j.gfs.2016.05.001.

Naylor, R.L., Hardy, R.W., Buschmann, A.H., Bush, S.R., Cao, L., Klinger, D.H., Little, D. C., Lubchenco, J., Shumway, S.E., Troell, M., 2021. A 20-year retrospective review of global aquaculture. Nature 591, 551–563. https://doi.org/10.1038/s41586-021-03308-6.

Naylor, R., Fang, S., Fanzo, J., 2023. A global view of aquaculture policy. Food Policy 116, 102422. https://doi.org/10.1016/j.foodpol.2023.102422.

Neumann, B., Vafeidis, A.T., Zimmermann, J., Nicholls, R.J., 2015. Future coastal population growth and exposure to sea-level rise and coastal flooding - a global assessment. PLoS One 10. https://doi.org/10.1371/journal.pone.0118571.

Otsu, N., 1979. A threshold selection method from gray-level histograms. IEEE Trans. Syst. Man Cybern. 9, 62–66.
Ottinger, M., Kuenzer, C., 2020. Spaceborne L-band synthetic aperture radar data for geoscientific analyses in coastal land applications: a review. Remote Sens. 12, 2228. https://doi.org/10.3390/rs12142228.
Ottinger, M., Clauss, K., Kuenzer, C., 2016. Aquaculture: relevance, distribution, impacts and spatial assessments – a review. Ocean Coast. Manag. 119, 244–266. https://doi.org/10.1016/j.ocecoaman.2015.10.015.
Ottinger, M., Clauss, K., Kuenzer, C., 2017. Large-scale assessment of coastal aquaculture ponds with Sentinel-1 time series data. Remote Sens. 9, 440. https://doi.org/10.3390/rs9050440.
Ottinger, M., Bachofer, F., Huth, J., Kuenzer, C., 2022. Mapping aquaculture ponds for the coastal zone of Asia with Sentinel-1 and Sentinel-2 time series. Remote Sens. 14, 153. https://doi.org/10.3390/rs14010153.
Prasad, K., Ottinger, M., Wei, C., Leinenkugel, P., 2019. Assessment of coastal aquaculture for India from Sentinel-1 SAR time series. Remote Sens. 11, 357. https://doi.org/10.3390/rs11030357.
Pueppke, S.G., Nurtazin, S., Ou, W., 2020. Water and land as shared resources for agriculture and aquaculture: insights from Asia. Water 12, 2787. https://doi.org/10.3390/w12102787.
Rahman, Md.T., Nielsen, R., Khan, Md.A., 2022. Pond aquaculture performance over time: a perspective of small-scale extensive pond farming in Bangladesh. Aquac. Econ. Manag. 26, 192–214. https://doi.org/10.1080/13657305.2021.1979122.
Ren, C., Wang, Z., Zhang, Y., Zhang, B., Chen, L., Xi, Y., Xiao, X., Doughty, R.B., Liu, M., Jia, M., Mao, D., Song, K., 2019. Rapid expansion of coastal aquaculture ponds in China from Landsat observations during 1984–2016. Int. J. Appl. Earth Obs. Geoinf. 82, 101902. https://doi.org/10.1016/j.jag.2019.101902.
Sampantamit, T., Ho, L., Lachat, C., Sutummawong, N., Sorgeloos, P., Goethals, P., 2020. Aquaculture production and its environmental sustainability in Thailand: challenges and potential solutions. Sustainability 12, 2010. https://doi.org/10.3390/su12052010.
Stiller, D., Ottinger, M., Leinenkugel, P., 2019. Spatio-temporal patterns of coastal aquaculture derived from Sentinel-1 time series data and the full Landsat archive. Remote Sens. 11, 1707. https://doi.org/10.3390/rs11141707.
Sun, Z., Luo, J., Yang, J., Yu, Q., Zhang, L., Xue, K., Lu, L., 2020. Nation-scale mapping of coastal aquaculture ponds with Sentinel-1 SAR data using Google earth engine. Remote Sens. 12, 3086. https://doi.org/10.3390/rs12183086.
Tian, P., Liu, Y., Li, J., Pu, R., Cao, L., Zhang, H., Ai, S., Yang, Y., 2022. Mapping coastal aquaculture ponds of China using sentinel SAR images in 2020 and Google earth engine. Remote Sens. 14, 5372. https://doi.org/10.3390/rs14215372.
Wang, Z., Zhang, J., Yang, X., Huang, C., Su, F., Liu, X., Liu, Y., Zhang, Y., 2022. Global mapping of the landside clustering of aquaculture ponds from dense time-series 10 m Sentinel-2 images on Google earth engine. Int. J. Appl. Earth Obs. Geoinf. 115, 103100. https://doi.org/10.1016/j.jag.2022.103100.
Wang, M., Mao, D., Xiao, X., Song, K., Jia, M., Ren, C., Wang, Z., 2023. Interannual changes of coastal aquaculture ponds in China at 10-m spatial resolution during 2016–2021. Remote Sens. Environ. 284, 113347. https://doi.org/10.1016/j.rse.2022.113347.
Xia, Z., Guo, X., Chen, R., 2020. Automatic extraction of aquaculture ponds based on Google earth engine. Ocean Coast. Manag. 198, 105348. https://doi.org/10.1016/j.ocecoaman.2020.105348.
Xu, H., 2006. Modification of normalised difference water index (NDWI) to enhance open water features in remotely sensed imagery. Int. J. Remote Sens. 27, 3025–3033. https://doi.org/10.1080/01431160600589179.
Ying, X., Ying, P., 2023. Analysis of green development of aquaculture in China based on entropy method. Sustainability 15, 5585. https://doi.org/10.3390/su15065585.
Zhang, X., Ma, S., Su, C., Shang, Y., Wang, T., Yin, J., 2020. Coastal oyster aquaculture area extraction and nutrient loading estimation using a GF-2 satellite image. IEEE J. Selected Top. Appl. Earth Observ. Remote Sens. 13, 4934–4946. https://doi.org/10.1109/JSTARS.2020.3016823.
Zhang, W., Belton, B., Edwards, P., Henriksson, P.J.G., Little, D.C., Newton, R., Troell, M., 2022. Aquaculture will continue to depend more on land than sea. Nature 603, E2–E4. https://doi.org/10.1038/s41586-021-04331-3.
Zhang, J., Yang, X., Wang, Z., Liu, Y., Liu, X., Ding, Y., 2023. Mapping of land-based aquaculture regions in Southeast Asia and its spatiotemporal change from 1990 to 2020 using time-series remote sensing data. Int. J. Appl. Earth Obs. Geoinf. 124, 103518. https://doi.org/10.1016/j.jag.2023.103518.
Zhe, S., Juhua, L., Jingzhicheng, Y., Li, Z., 2020. Dynamics of coastal aquaculture ponds in Vietnam from 1990 to 2015 using Landsat data. IOP Conf. Ser.: Earth Environ. Sci. 502, 012029. https://doi.org/10.1088/1755-1315/502/1/012029.